EUROPEAN SOUTHERN OBSERVATORY

Organisation Européene pour des Recherches Astronomiques dans l'Hémisphère Austral
Europäische Organisation für astronomische Forschung in der südlichen Hemisphäre

ESO - European Southern Observatory
Karl-Schwarzschild Str. 2, D-85748 Garching bei München

Very Large Telescope
Paranal Science Operations
VISIR User Manual

Doc. No. VLT-MAN-ESO-14300-3514

Issue 79, Date 30/11/2006

Prepared A. Smette,L. Vanzi . . . . . .
Date Signature

Approved A. Kaufer . . . . . .
Date Signature

Released O. Hainaut . . . . . .
Date Signature

This page was intentionally left blank

Change Record

Issue/Rev.	Date	Section/Parag. affected	Reason/Initiation/Documents/Remarks
1.0	04/09/04	creation	First release for science verification in P74 and OT proposals in P75.
1.1	10/12/04	2.4, 3.2, 6.2, 6.3, 7, 8	update for P75 Phase2
v76.1	01/02/05	all	update for P76 CfP
v76.2	06/07/05	all	update for P76 Phase 2
v76.3	14/07/05	4.8.1	Corrected Legend Fig 17
v76.4	14/07/05	Cover pages	Corrected typos
v77.1	04/09/05	3.5,3.6,3.7,4.1,4.3,4.8.1,7,8.1,10	update for P77 CfP
v77.2	05/09/05	4.6	match imager overhead of CfP
v77.3	20/12/05	1,2,3.4,3.6,4.2-4.4,4.7,7,8	update for P77 Phase2
v78.1	27/02/06	3.6, 3.10	update for P78 CfP
v78	19/06/06	cover, 2.2, 3.2, 4.3.1	P78 release
v79	30/11/06	4.8	P79 release
v1.0, v1.1, v76.1: edited by R. Siebenmorgen, E. Pantin, M. Sterzik v76.2–4, v77.1-3, updated by A. Smette.			

Contents

1 Introduction **1**

2 Observing in the MIR from the ground **1**
2.1 The Earth's atmosphere . . . 1
2.2 The spatial resolution . . . 2
2.3 MIR background . . . 2
2.4 Chopping and nodding . . . 3
2.5 Sensitivity . . . 6

3 Instrument description and offered observing modes **6**
3.1 Imager . . . 6
3.2 Spectrometer . . . 10
3.2.1 Slit widths . . . 11
3.2.2 Resolution . . . 11
3.2.3 Low resolution: offered central wavelengths . . . 11
3.2.4 Medium resolution: offered central wavelengths . . . 12
3.2.5 High resolution: offered central wavelengths . . . 12
3.3 Calibration units . . . 13
3.4 Detectors . . . 13
3.5 Data acquisition system . . . 15

4 Observing with VISIR at the VLT **18**
4.1 Proposal preparation . . . 18
4.2 Telescope observing parameters . . . 20
4.2.1 Instrument orientation on the sky . . . 20
4.2.2 Chopping parameters . . . 20
4.2.3 Nodding parameters . . . 21
4.3 Target acquisition . . . 22
4.3.1 Introduction . . . 22
4.3.2 Description . . . 22
4.4 Guide stars . . . 25
4.5 Brightness limitations . . . 26
4.6 Overheads . . . 26
4.7 Calibration observations . . . 27
4.8 OBs Classification . . . 28
4.9 Known problems . . . 29
4.9.1 Decreased image quality . . . 29
4.9.2 Low–level stripes . . . 30
4.9.3 Bad residuals . . . 30
4.9.4 Residuals of sky emission lines . . . 30

4.9.5 Fringes 30

5 VISIR data **31**
5.1 Data format 31
5.2 Pipeline 31
5.3 VISIR spectrometer data 32

6 VISIR templates description **34**
6.1 Acquisition 34
6.2 Observing with the imager 34
6.3 Observing with the spectrometer 36
6.4 Calibration 37

7 Checklist **38**
7.1 Phase 1 38
7.2 Phase 2 38

8 Appendix: VISIR template parameters **41**
8.1 Acquisition 41
8.2 Observation 44
8.3 Calibration 47

9 Appendix: Filter transmission curves **49**

10 Appendix: Observed sensitivities in various spectroscopic settings **52**

List of acronyms

BIB	Blocked impurity band
BLIP	Background limited performance
BOB	Broker of observation blocks
DIT	Detector integration time
ETC	Exposure time calculator
FWHM	Full width at half maximum
ICS	Instrument control software
IR	Infrared
IRACE	Infrared array control electronics
MIR	Mid infrared
OB	Observing block
P2PP	Phase 2 proposal preparation
PAE	Preliminary acceptance in Europe
pfov	pixel field of view
PSF	Point spread function
S/N	Signal–to–noise ratio
UT	Unit telescope
VISIR	VLT imager and spectrometer for the mid infrared
TCS	Telescope control system
TMA	Three mirrors anastigmatic
WCU	Warm calibration unit

1 Introduction

The VLT spectrometer and imager for the mid–infrared (VISIR), built by CEA/DAPNIA/SAP and NFRA/ASTRON, provides diffraction–limited imaging at high sensitivity in two mid-infrared (MIR) atmospheric windows: the N-band between $\approx$ 8 to 13 μm and the Q-band between 16.5 and 24.5 μm. In addition, it offers a slit spectrometer with a range of spectral resolutions between 150 and 30000.

The MIR provides invaluable information about the warm dust and gas phase of the Universe. Micron sized particles such as silicates, silicon carbide, carbon, coals, aluminum oxides or polycyclic aromatic hydrocarbon (PAH) molecules are major contributors to the thermal MIR emission. The gaseous phase emits through a large number of ionic and atomic lines. Examples are NeII (12.8 μm) and the pure rotation lines of molecular hydrogen at 8.02, 9.66, 12.27 and 17.03 μm .

Because of the very high background from the ambient atmosphere and telescope, the sensitivity of ground–based MIR instruments cannot compete with that of space–born ones. However, ground based instruments mounted on large telescopes offer superior spatial resolution. For example VISIR at the VLT provides diffraction limited images at $\sim 0.3''$ (FWHM) in the N band. This is an order of magnitude better than what can be reached by the Spitzer Space Telescope (SST).

The VISIR user manual is structured as follows: Basic observing techniques of ground–based MIR instruments are summarized in §2. §3 provides a technical description of VISIR and its offered observing modes offered. An overview on how to observe with VISIR at the VLT can be found in § 4. A description of the structure of the imaging and spectroscopic data files is given in § 5. A checklist to help the preparation of OBs is available in § 7. Acquisition, observing and calibration templates are explained in § 6.

We strongly recommend to consult:
http://www.eso.org/instruments/visir/ for additional information and updates. For support during proposal preparation and OB submission, please contact ESO's User Support Department (usd-help@eso.org).

2 Observing in the MIR from the ground

2.1 The Earth's atmosphere

Our atmosphere absorbs the majority of the MIR radiation from astronomical sources. The main absorbing molecules are H_2O, CH_4, CO_2, CO, O_2, O_3. However, the atmosphere is quite transparent in two atmospheric windows: the N and Q bands. They are centered around 10 and 20 μm, respectively. The transmission in the N band is fairly good at a dry site and becomes particular transparent in the wavelength range 10.5-12 μm . However, the transmission of the Q band is rapidly decreasing with wavelength and can be viewed as the superposition of many sub–bands having a typical spectral coverage of $\Delta\lambda = 1\mu$m at an average transmission of 60%. Observations in this band require low water vapor content in the atmosphere. The atmospheric transmission in the N and Q bands is displayed on Fig. 1.

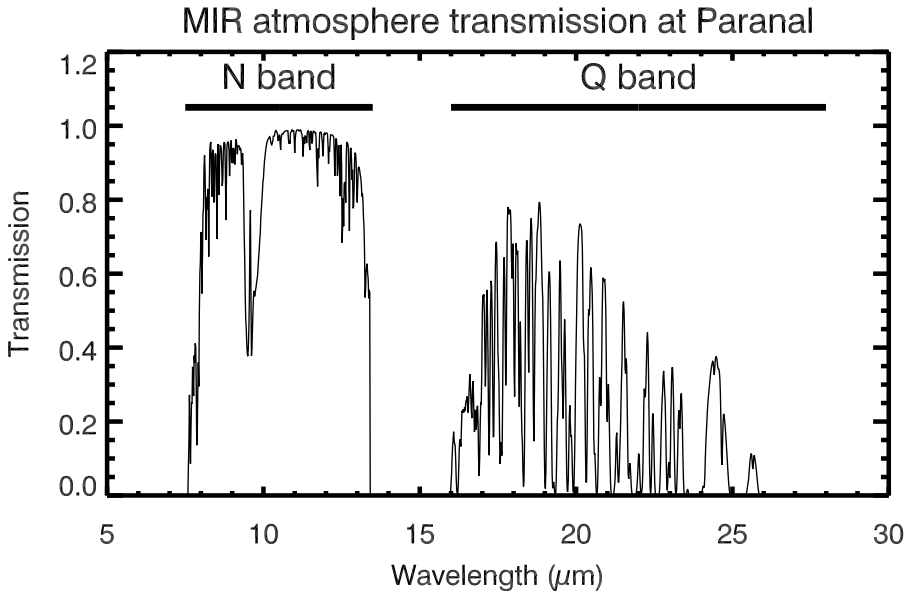

Figure 1: MIR atmospheric transmission at Paranal computed with HITRAN for an altitude of 2600 m and 1.5 mm of precipitable water vapor at zenith. The US standard model atmosphere is used.

2.2 The spatial resolution

The spatial resolution of an instrument is ultimately limited either by the diffraction of the telescope or the atmospheric seeing. The diffraction limit as measured by the diameter of the first Airy ring increases with wavelength as $1.22\ \lambda/D$, where λ is the observing wavelength and D the diameter of the telescope mirror (see solid line in Fig. 2). The wavelength dependence of the seeing can be derived by studying the spatial coherence radius of the atmosphere in the telescope beam and is to first order approximated by the Roddier formula, where the seeing is $\propto \lambda^{-0.2}$ (see dot-dashed lines in Fig. 2). However, initial results from VISIR data indicate that this formula overestimates the measured MIR seeing at Paranal by 20–50%, as the size of a UT mirror is comparable to the turbulence outer scale. As a result, VISIR data are already diffraction limited for optical seeing below 0.6″. The results of measures obtained in 2005 are shown in Fig. 3.

2.3 MIR background

The atmosphere does not only absorb MIR photons coming from astrophysical targets, but also emits a strong background with the spectral shape of a black-body at about 253 K (Kirchhoff's law). The telescope gives an additional MIR background. The VLT telescopes emits at 283 K with a preliminary emissivity estimate of $< 15\%$ in N. The VISIR instrument is cooled to avoid internal background contamination. The detectors are at $\sim 5-6$ K and the interior of the cryostat at 33 K. The background radiation at 10μm is typically $m_N = -5$ mag/arcsec^2 (3700 Jy/arcsec^2) and at 20μm $m_Q = -7.3$ mag/arcsec^2 (8300 Jy/arcsec^2).

Consequently, the number of photons reaching the detector is huge, often more than 10^8 photons/s. Therefore, the exposure time of an individual integration - the Detector Integration Time (DIT) – is short, of the order of a few tens of milli–seconds in imaging mode.

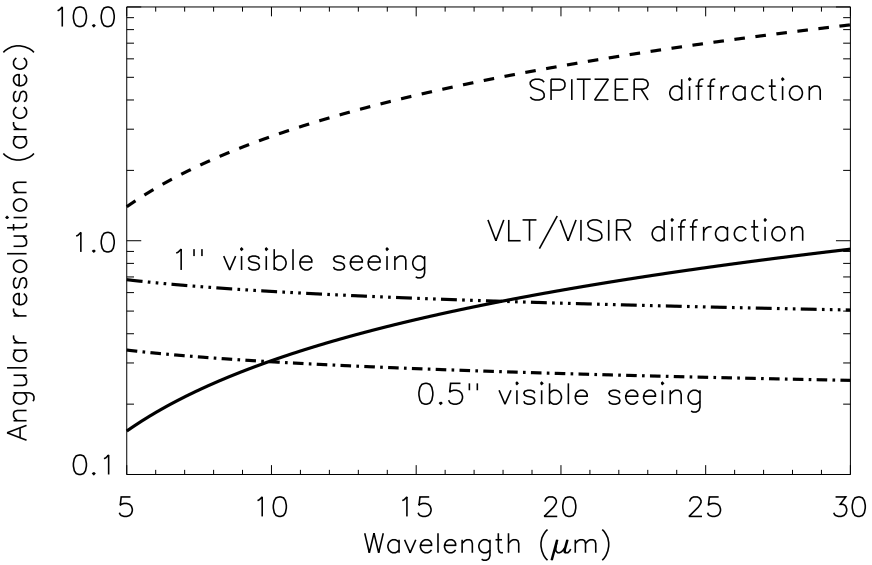

Figure 2: VLT diffraction limit (full line) versus seeing. The Spitzer Space Telescope diffraction limits (dashed) are shown for comparison. The Roddier dependence is shown for two optical seeings (dashed-dot).

2.4 Chopping and nodding

The basic idea to suppress the MIR background is to perform differential observations, using the chopping/nodding technique.

In the chopping technique two observations are performed. One set of exposures on–source, include the background and the astronomical source. A second set of off-source exposures measures the pure background. The on– and off–source observations have to be alternated at a rate faster than the rate of the background fluctuations. In practice, it is achieved by moving the secondary mirror of the telescope. For VISIR at Paranal, a chopping frequency of 0.25 Hz has been found to be adequate for N-band imaging observations, while 0.5 Hz are adopted for Q-band imaging. Spectroscopic observations are performed with lower chopper frequencies, at 0.1 Hz or less.

The chopping technique cancels most of the background. However, the optical path is not exactly the same in both chopper positions. Therefore a residual background remains. It is varying at a time–scale which is long compared to that of the sky. This residual is suppressed by nodding, where the telescope itself is moved off–source and the same chopping observations as in the on–source position is repeated.

An illustration of the chopping and nodding technique is shown on Fig. 4. Depending on the choice of chopping and nodding amplitudes and directions, up to 4 images of the source can be seen on the frame and used for scientific analysis. Of course, the *free* field–of–view on the chop/nod images can be severely reduced depending on the particular chopping and nodding parameters chosen.

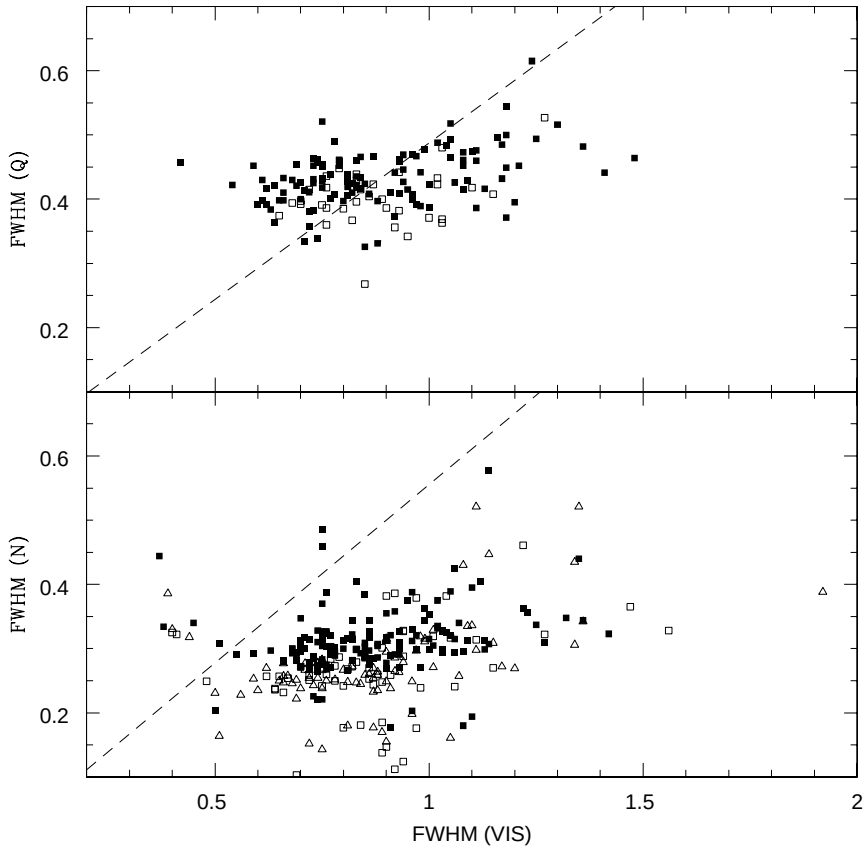

Figure 3: Measures of the VISIR image quality versus optical seeing obtained during 2005. The dashed lines indicates the prediction of Roddier's formula.

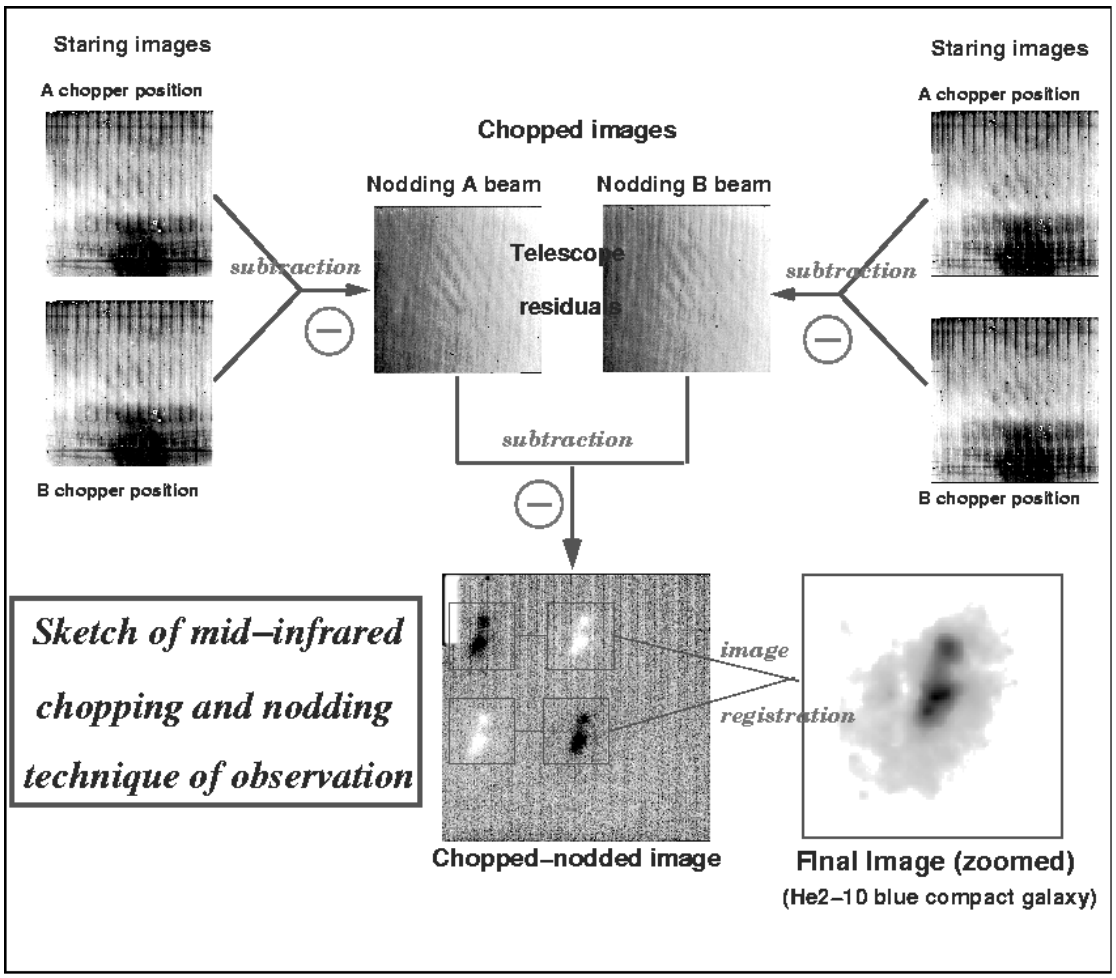

Figure 4: Illustration of the chopping and nodding technique on observations of the blue compact galaxy He2-10. The galaxy only appears after chopping and nodding (courtesy VISIR commissioning team, June 2004).

2.5 Sensitivity

Measurements of VISIR sensitivities are based on observations of mid–infrared calibration standard stars (Cohen et al. 1999, AJ 117, 1864). In imaging mode, the stars are recorded in the small field (0.075″) and intermediate field (0.127″) by perpendicular chopping and nodding patterns with amplitudes of 10″. Calibrators are frequently observed during the night (§4.7). Flux and noise levels are extracted by multi–aperture photometry using the curve–of–growth method: the aperture used for all 4 beams in a given frame is the one for which the flux to noise ratio is the largest. By combining all 4 beams, *the sensitivity in a given set–up (filter, field of view) is defined as the limiting flux of a point–source detected with a S/N of 10 in one hour of on–source integration.*

The growing calibration database allows a statistical analysis of the sensitivity with respect to instrumental and atmospherical conditions. The values for each filter given in Table 2 refer to the median of more than 600 different observations during September and December 2004. A graphical compilation is presented in Fig. 5 for the N-band and Q-band imaging filters. Some of the best measurements approach theoretical expectations, i.e. they are close to background limited performance (BLIP).

Sensitivity estimates for the VISIR spectroscopy observing modes are obtained in a similar way. However, in this case, chopping and nodding are executed in parallel. Consequently, only 3 beams are obtained, with the central one containing twice as much flux as the two other ones.

Table 4 to 6 list typical sensitivities measured in low, medium and high resolution modes away from strong sky emission lines for the wavelength ranges offered in P76. Figures 20 to 36 in the Appendix (§ 10) shows the dependence of sensitivity on wavelength.

The median sensitivities are the reference for classification of VISIR service mode observations, and the basis to assess the feasibility of an observing programme. In particular, *classification* of service mode OBs will be based on sensitivity measurements made at zenith. Calibrations will be provided following the guidelines given in § 4.7. For up to date information, please consult http://www.eso.org/instruments/visir. The use the VISIR exposure time calculator (ETC, located at http://www.eso.org/observing/etc/) is recommended to estimate the on–source integration time.

3 Instrument description and offered observing modes

VISIR offers two spatial scales in imaging and several spectral resolution modes in slit spectroscopy. The imager and spectrograph are two sub–instruments. They have independent light paths, optics and detectors. The cryogenic optical bench is enclosed in a vacuum vessel. The vessel is a cylinder, 1.2 m long and 1.5 m in diameter. Standard Gifford–McMahon closed–cycle coolers are used to maintain the required temperature: 33 K for most of the structure and optics and < 15 K for the parts near the detector. The detectors are cooled down to $\sim 5 - 6$ K.

3.1 Imager

The imager is based on an all–reflective design. The optical design is shown in Fig. 6. It consists of two parts:

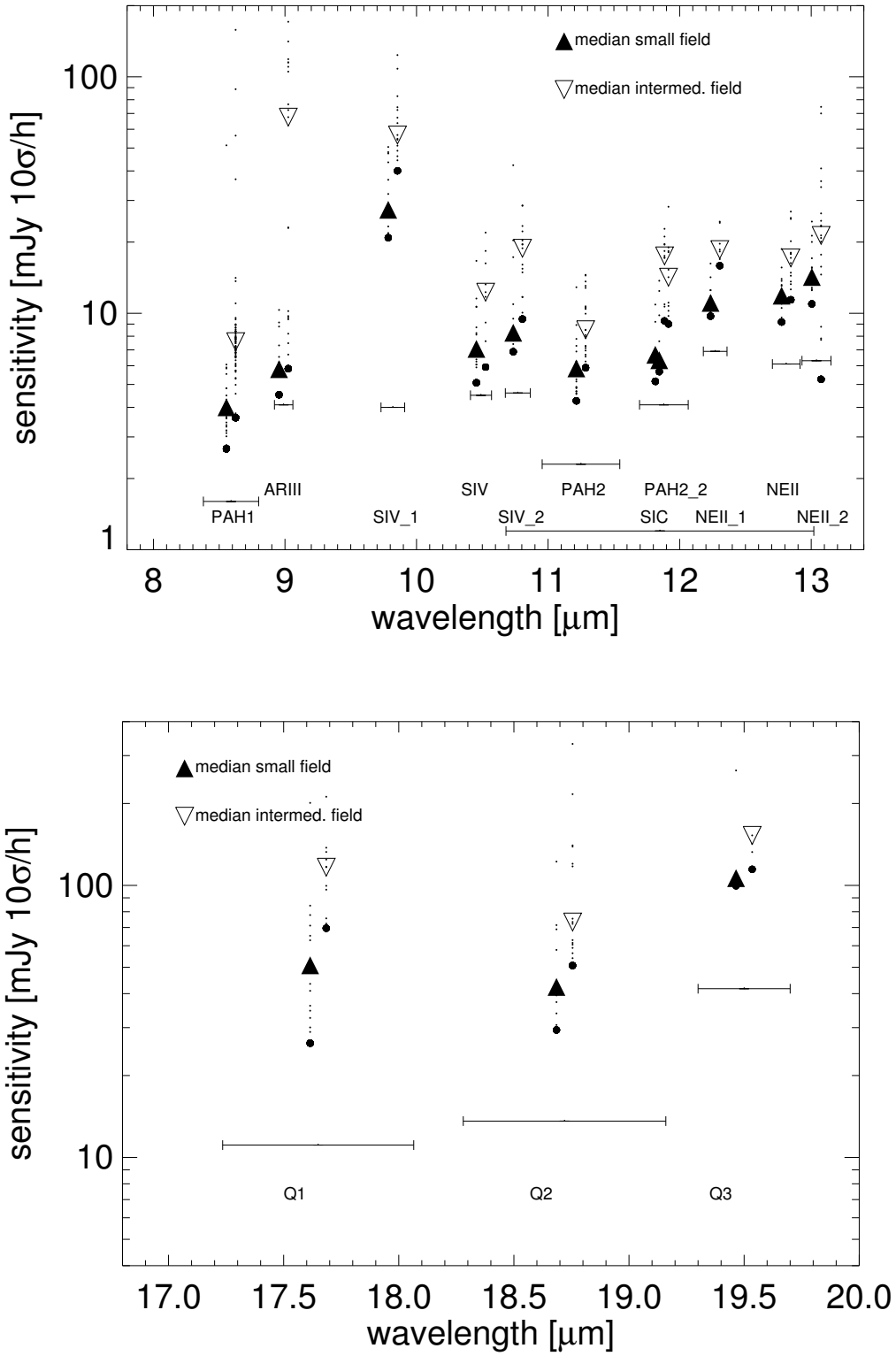

Figure 5: Sensitivities for the VISIR imager for the N (top) and Q-band (bottom). Small and intermediate field observations are displaced for clarity. Background noise limits are indicated for the individual filter bandpasses.

- A collimator, which provides an 18 mm diameter cold stop pupil in parallel light: As generally designed for IR instruments, the pupil of the telescope is imaged on a cold stop mask to avoid straylight and excessive background emission. The collimator mirror (M1) is a concave aspherical mirror. It is followed by a folding flat mirror (M2) which eases the mechanical implementation.

- A set of three objectives mounted on a wheel. Each objective is based on a three mirror anastigmatic (TMA) system. Each of the TMA's is made of three conic mirrors.

The 0.075″ (small field, SF) and 0.127″ (intermediated field, IF) pixel scale are offered (Table 1). These offered pixel fields of view (pfov) ensure a proper sampling of the images in the N and Q-band.

pfov	fov	diffraction[a] μm	diffraction[a] pixels
0.127″	32.5″ × 32.5″	94	1.88
0.075″	19.2″ × 19.2″	159	3.18

[a] Radius of first Airy ring at λ=7.7μm

Table 1: VISIR imager pixel scales offered. The pixel size of the DRS 256x256 detector is 50 μm . The first airy ring at λ=7.7μm corresponds to a radius of 0.24″on the sky.

The filter wheel is located just behind the cold stop pupil mask. The list of filters offered is given in Table 2. The transmission curves of the filters measured at 35 K are plotted in the Appendix.

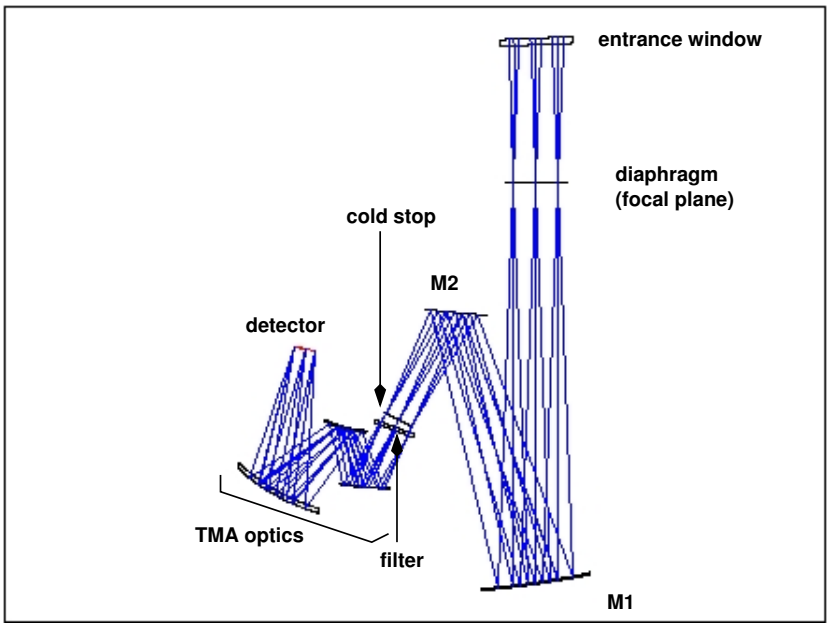

Figure 6: The optical path of the imager in the intermediate field (0.127″/pixel) is shown from the entrance window down to the detector.

filter	λ_c (μm)	half–band width (μm)	maximum transmission (%)	sensitivity (mJy 10σ/1h) theory (BLIP)	median SF	median IF
PAH1	8.59	0.42	77	1.6	5	8
ArIII	8.99	0.14	72	4.1	6	70
SIV_1	9.82[1]	0.18	72	4.0	30	60
SIV	10.49	0.16	70	4.5	8	13
SIV_2	10.77[1]	0.19	70	4.6	9	20
PAH2	11.25	0.59	75	2.3	6	9
SiC	11.85	2.34	75	1.2	7	18
PAH2_2	11.88[1]	0.37	58	4.1	7	15
NeII_1	12.27[1]	0.18	51	6.9	12	20
NeII	12.81	0.21	64	6.1	12	18
NeII_2	13.04	0.22	68	6.3	15	22
Q1	17.65	0.83	59	11.1	50	120
Q2	18.72	0.88	49	13.6	50	80
Q3	19.50	0.40	50	41.7	100	160

Table 2: VISIR imager filter characteristics, following the manufacturer specifications, except for the central wavelengths noted with [1] which were re-determined with a monochromator and the WCU because they deviate from specifications. The last 3 columns give, respectively, the theoretical expectations under BLIP and excellent weather conditions, and the measured median sensitivities for the Small and Intermediate Field obtained in various weather conditions. The measured sensitivities were obtained using the curve–of–growth method on data obtained in perpendicular chopping/nodding directions (4 beams).

3.2 Spectrometer

VISIR offers slit spectroscopy at three spectral resolutions with a pixel scale of 0.127″. This is obtained by means of two arms, one with low order gratings for the low and medium spectral resolution, the other with large echelle gratings providing high spectral resolution.

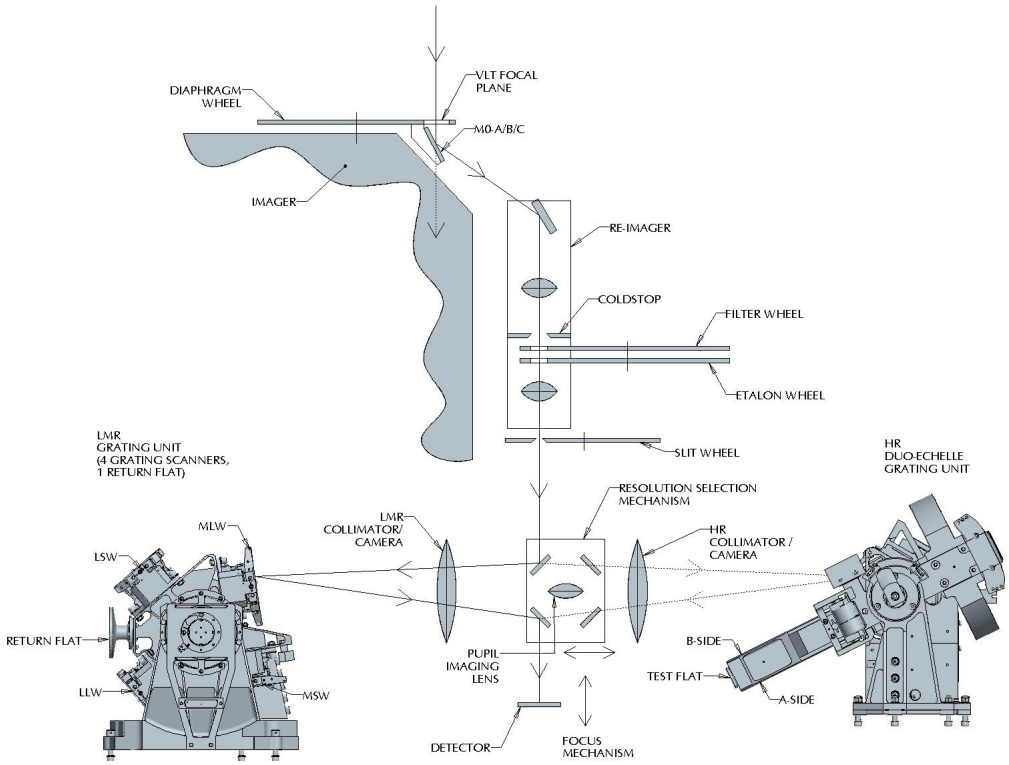

Figure 7: Schematic layout of the design of the VISIR spectrometer.

The long slits have a length of 32.5″and therefore cover the whole width of the detector. The short slits, only used in high–resolution cross–dispersed mode, have a length of 4.1″. The all-reflective optical design of the spectrometer uses two TMA systems in double pass (pass 1: collimator, pass 2: camera). A schematic layout of the VISIR spectrometer design is shown in Fig. 7. The 3–mirror system of the low– and medium–resolution arm gives a 53 mm (diameter) collimated beam; the collimated beam diameter in the high-resolution arm is 125 mm. Both subsystems image the spectrum onto the same detector; selection between the two spectrometer arms is done by two pairs of folding flat mirrors. In front of the actual spectrometer subsystems is a reflective re–imager consisting of two off–axis paraboloids and three folding flats. The re–imager provides a 16 mm diameter cold-stop pupil in parallel light and transforms the incoming VLT Cassegrain beam of F:13.4 to an F:10 beam at the spectrometer entrance. The spectrometer slit wheel is also equipped with a very wide slit (15.3″) named OPEN in P2PP. It gives the possibility to make imaging with the spectrometer detector and is used for object acquisition and centering on the detector.

The list of available filters for spectroscopic acquisition offered is given in Table 3, together with their measured bandpasses and approximate sensitivities for image acquisition.

filter	λ_c (μm)	half–band width (μm)	sensitivity (mJy/10σ/1h)
N_SW	8.85	1.35	40
N_LW	12.1	1.9	40
ArIII	8.94	0.11	200
NeII_1	12.35	0.50	80
NeII_2	12.81	0.10	50

Table 3: VISIR spectrometer filter characteristics. The filters transmissions have been determined with a monochromator and the WCU. The last column list the measured median sensitivities which were obtained using the curve–of–growth method on data obtained in parallel chopping/nodding directions (3 beams).

3.2.1 Slit widths

Three different slit widths (0.4″, 0.75″and 1″) are offered for all settings. For over-sized widths (e.g. for the 1″slit with respect to the diffraction limit around 10μm) the spectral resolution of a point–source spectrum is better than the one of the sky spectrum; in addition, the zero–point of the wavelength calibration will be affected by an incorrect centering of the object within the slit.

3.2.2 Resolution

In the N band, the low–resolution and medium resolution modes provide spectral resolving power of $\sim$ 300 (Table 4) and $\sim$3000 (Table 5), respectively. In high resolution long–slit mode, narrow wavelength ranges around the 8.02 [H2_S4], 12.813 [Ne II] and 17.03 μm [H2_S1] line are offered. With the 1″slit the measured spectral resolution is $R \sim 15000$ (Table 6), and a minimum flux in an emission line below 10^{-16} W/m^2/arcsec^2 can be achieved. This value corresponds to an approximate sensitivity limit around 1 Jy in the continuum. A high–resolution, cross–dispersed mode with a 4.1″ short slit is available for a number of wavelength settings (Table 6).

Please consult http://www.eso.org/instruments/visir for the latest update of the list of offered modes and slits.

3.2.3 Low resolution: offered central wavelengths

The 'clean' part of the N–band can be covered in 4 settings with central wavelengths 8.8, 9.8, 11.4 and 12.4 μm . Two additional settings at 8.5 and 12.2 μm are offered as alternative to the 8.8 and 12.4 μm settings, respectively, mostly for cosmetic reason, as they avoid strong sky emission lines to fall on bad pixels. Indeed, the 8.5μm setting moves the blue wing of the ozone band off the wavelength range covered by the detector, at the expense of having a larger part of the detector covering the red wing of the water-vapour band. The 12.2μm setting avoids the CO2 band.

Additionally, a bluer setting, centered at 8.1 μm covers the spectral range down to the transmission cut–off at 7.1μm . It aims at covering the 7.6 μm methane band and 7.7 μm PAH feature.

In all cases, classification of OBs in service mode will be based on the clean parts of the spectra. Note that the exposure time calculator (ETC) cannot currently provide sensitivity estimates for $\lambda < 7.6\mu$.

λ – range (μm)	λ_c (μm)	grating order	spect.–resol. (measured, 1″slit)	dispersion (pixels/μm)
7.1-8.7	8.1	2	300 – 390	160.02
7.7-9.3	8.5	2	300 – 390	160.02
8.0-9.6	8.8	2	300 – 390	160.02
9.0-10.6	9.8	2	305 – 360	160.05
10.34-12.46	11.4	1	185 – 220	119.94
11.14-13.26	12.2	1	215 – 250	119.96
11.34-13.46	12.4	1	215 – 250	119.96

Table 4: VISIR low resolution offered settings. The first column gives the wavelength range of a spectrum for the central wavelength (λ_c) listed in the 2nd column. The measured sensitivities are ~ 50 mJy at 10σ/1h in the clean regions of the spectrum (cf. Fig. 20) for a slit width of 1″. Offered slits have widths of 0.40, 0.75 and 1.00″. The spectral resolution of the 8.1μm , 8.5μm and 12.2μm settings has not been independently measured; values for the 8.8μm and 12.4μm settings are reported instead.

3.2.4 Medium resolution: offered central wavelengths

In Medium Resolution mode, the central wavelength λ_c can be freely chosen within the wavelength ranges listed in Table 5. Note that the exposure time calculator (ETC) cannot currently provide estimates of S/N for $\lambda < 7.6\mu$m . Table 5 provides offered sensitivities.

λ_c – range (μm)	$\Delta\lambda$ (μm)	grating order	spect.–resol. (measured, 1″slit)	dispersion (pixels/μm)	sensitivity (mJy at 10σ in 1h)
7.5 – 8.0	0.195	2	~ 3500	~ 1315	1000
8.0 – 9.3	0.188	2	~ 3500	~ 1360	200
10.2 – 13.0	~ 0.21	2	~ 3500	$\sim 1450 - 1040$	200
17.1 – 19.0	0.37	1	~ 1800	~ 695	1200
20.12	0.36	1	~ 1800	720	2000

Table 5: VISIR medium resolution settings. The first column gives the minimum and maximum allowed values for the central wavelength (λ_c) in the given setting. The wavelength range per setting in given in the 2nd column ($\Delta\lambda$). The spectral resolution, measured with a 1″slit, is given in the 3rd column. The dispersion is given in the 4th column. Typical offered sensitivites are given in the last column. Examples of dependence of sensitivity with wavelength are shown in Figures 21 to 24. Offered slits have widths of 0.40, 0.75 and 1.00″.

3.2.5 High resolution: offered central wavelengths

The VISIR spectrometer offers a high–resolution long–slit mode for 3 passbands centered in the wavelengths of the [H2_S4], [NeII] and [H2_S1] lines. A wider range of wavelengths is accessible with the high–resolution cross–dispersed mode, with a 4.1″ long slit.

Offered modes and sensitivities are given in Table 6. The ETC offers the possibility to take into account the earth motion to predict the observed wavelength of a given line depending on the foreseen date and time of observations. In particular, this feature allows to determine the dates when the emission line under study would appear at the same wavelength as a sky line.

mode	λ_c (μm)	$\Delta\lambda$ (μm)	line	order	R	dispersion (pixels/μm)	sensitivity Jy 10σ/1h
HR	7.970 – 8.270	0.02420	[H2_S4]	17B	32000	10544	∼3
HR	12.738 – 12.882	0.03571	[Ne II]	11A	17000	7145	∼0.9
HR	16.800 – 17.200	0.05156	[H2_S1]	8B	14000	4950	<10
HRX	8.970 – 9.140	0.02270	[ArIII]	16A	27100	11194	∼ 4
HRX	9.360 – 9.690	0.02325	[H2_S3]	15A	25000	10974	∼5
HRX	10.480 – 10.540	0.03160	[SIV],[CoII]	12B	24000	8044	∼4
HRX	11.540 – 11.570	0.03210	HD (0,0) R(10)	12B	23400	8000	∼ 2
HRX	11.762	0.03260	[ClIV]	12A	19100	7840	∼ 3
HRX	12.210 – 12.760	0.03864	[H2_S2]	11B	20000	6604	∼1.5
HRX	12.814 – 13.364	0.03550	[NeII]	11A	17500	7150	∼2
HRX	16.390	0.03551	[CoIII]	9A	17300	7260	∼ 12
HRX	16.925	0.05240	[CoI]	8B	14100	4840	∼ 8
HRX	17.790 – 17.980	0.04707	[PIII],[FeII]	8A	13140	5400	∼ 4
HRX	18.246	0.04182	[NiII]	8A	14600	6080	∼ 8
HRX	18.680 – 18.960	0.06569	[SIII]	7B	11150	3870	∼ 4
HRX	21.295	0.04196	[NaIV]	7A	14300	6058	∼ 9

Table 6: VISIR high resolution long–slit (HR) and cross-dispersed (HRX) modes. The second column gives the minimum and maximum allowed values for the central wavelength (λ_c) in the given setting. The wavelength range per setting in given in the 3rd column ($\Delta\lambda$). R is the theoretical spectral resolution. Offered slits have widths of 0.40, 0.75 and 1.00″. Note that the range 12.210 – 12.760 also covers HD (0,0) R(9), while the [NeII] emission line can be observed up to $z \approx 0.038$.

3.3 Calibration units

A warm calibration unit (WCU) is located on top of the VISIR vacuum enclosure. The WCU is also called star simulator. It simulates either a monochromatic point source with adjustable wavelength or an extended black-body source with adjustable temperature. A selection mirror allows to switch from the telescope to the simulator beam. It can be used for calibration and tests, also during daytime. Fig. 8 shows the unit on top of the enclosure.

3.4 Detectors

The VISIR imager and spectrometer are each equipped with a DRS, former Boeing, 256×256 BIB detector. The quantum efficiency of the detectors is greater than 50% and reaches 65% or more at 12 μm (Fig. 9).

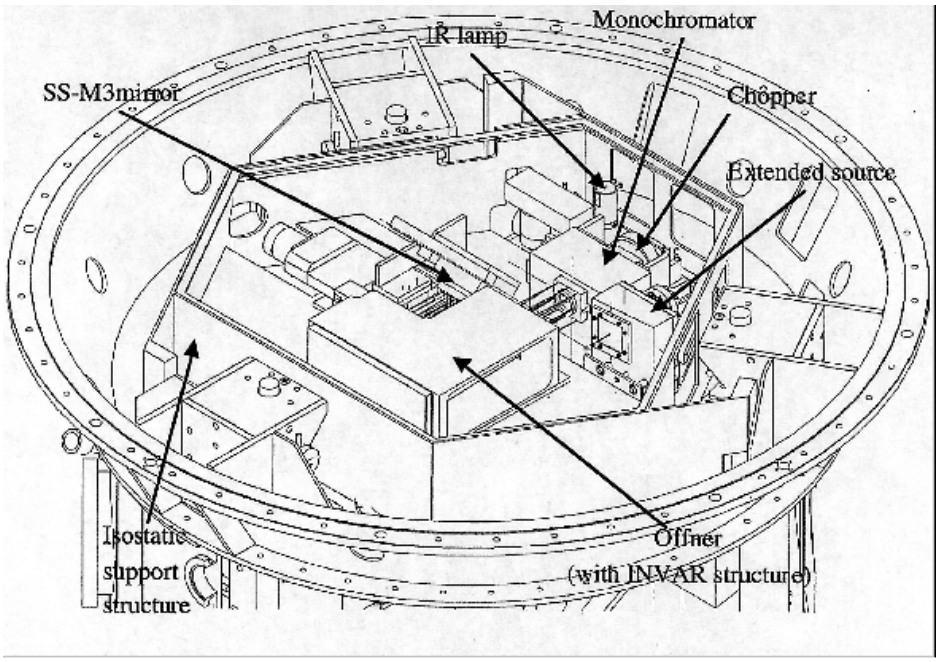

Figure 8: Schematic drawing of the warm calibration unit on top of the VISIR vessel.

The detector noise has to be compared with the photon noise of the background. As shown in Fig. 10, the measured noise in an observation consists of read–out noise and fixed pattern noise, which are both independent of the detector integration time (DIT). At the operating temperature of the detector ($\sim$ 6 K), the dark current, which is the signal obtained when the detector receives no photons, is negligible compared to the background generated by the photons emitted by the telescope and the atmosphere. The dark current is removed by the observation technique (chopping or nodding). It is at least 6 times lower than the photon noise for the spectrometer and negligible for the imager.

The detectors have a switchable pixel ("well") capacity. The large capacity is used for broad-band imaging and the small capacity for narrow band imaging and spectroscopy. Detector saturation due to the enormous MIR background is avoided by a storage capacity of $1.9 \cdot 10^6$ e^- in small and $1.8 \cdot 10^7$ e^- in large capacity modes, respectively. For background limited noise performance (BLIP), the optimal operational range of the detector is half of the dynamic range for the large capacity, and between 1/2 and 1/5 for the small capacity. The detector is linear over 2/3 of its dynamic range (Fig. 11) and its working point is set in the middle of the dynamic range. During commissioning it was found that, for about half of the array, the gain does not differ by more than 2% peak-to-peak. By comparison with other limitations, flat-field corrections, which are difficult to implement in the MIR, are not considered important. The detector integration time (DIT) is a few milli–seconds in broad-band imaging and may increase to $\sim$ 2 s in high resolution spectroscopy. The DIT is determined by the instrument software according to the filter and pfov. It is not a parameter to be chosen by the observer.

The DRS detectors contain a fair fraction of bad pixels ($< 2\%$, Fig.12). The imager detector suffers from striping and appearances of ghosts. The relatively wide rectangular area in the lower right corner (South–West corner for PA = 0 deg) of the imager detector or some other rectangular areas are masked out to avoid such disturbances (Fig. 13). For bright objects the DRS detector shows memory effects. Stabilization is ensured by introducing dead times where necessary. It is advised to observe only sources fainter than 500 Jy in N and 2500 Jy in Q.

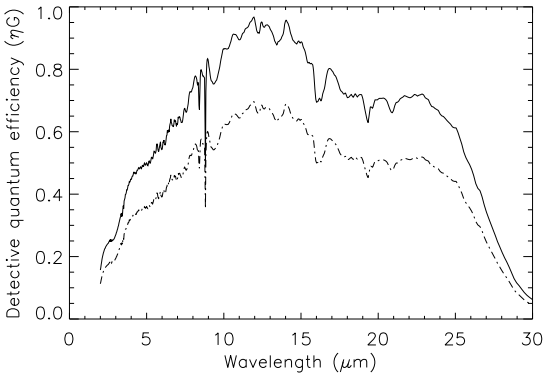

Figure 9: Detector quantum efficiency at 12 K provided by DRS (solid line). The same curve (dashed) but scaled by 0.72 reflects a lower limit of the quantum efficiency. The scaling was derived from laboratory measurements. Note the sharp absorption feature at 8.8 μm that will appear in raw spectroscopic data.

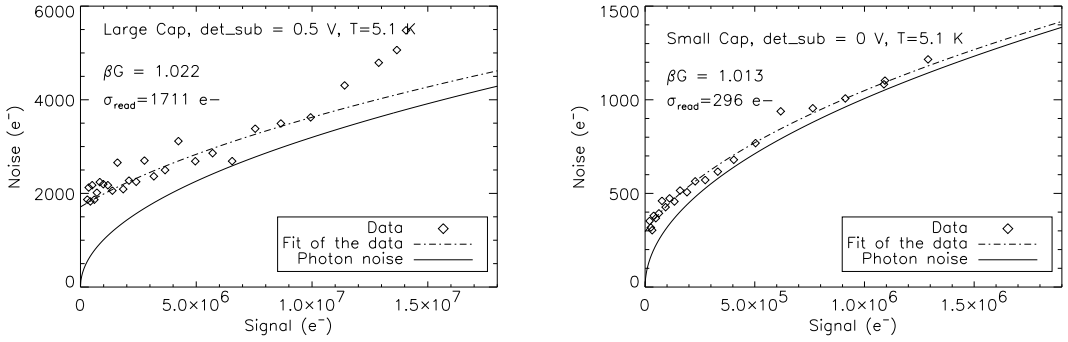

Figure 10: Noise as a function of the incoming flux in the large (left) and small (right) capacity mode. Superimposed is the theoretical photon noise. BLIP performances are approached for higher fluxes and larger DIT, respectively.

These artifacts are less important in spectroscopy due to the lower light levels but clearly visible on objects brighter than $\sim 2\%$ of the background. However, a `TEL.CHOP.THROW` between 9 to 13″ shoud be avoided, in particular for objects bright enough to be seen in individual DITs, as one of the beams will hit some particularly hot pixels in the lower–left of the spectrometer detector (see Fig.14).

3.5 Data acquisition system

Both VISIR detectors are controlled by the ESO standard IRACE acquisition system. In imaging the read–out rate of the detector is high. Up to 200 frames per s are read for a minimum detector integration time of DIT= 5 ms. Such a frame rate is too high to store all exposures. One VISIR image is of size 256x256; each pixel is coded with 4 bytes (long integer). Thus one read–out has a size of 262 kB. During each chopping cycle the elementary exposures are added in real time and only the result is stored on disk. At a chopping frequency

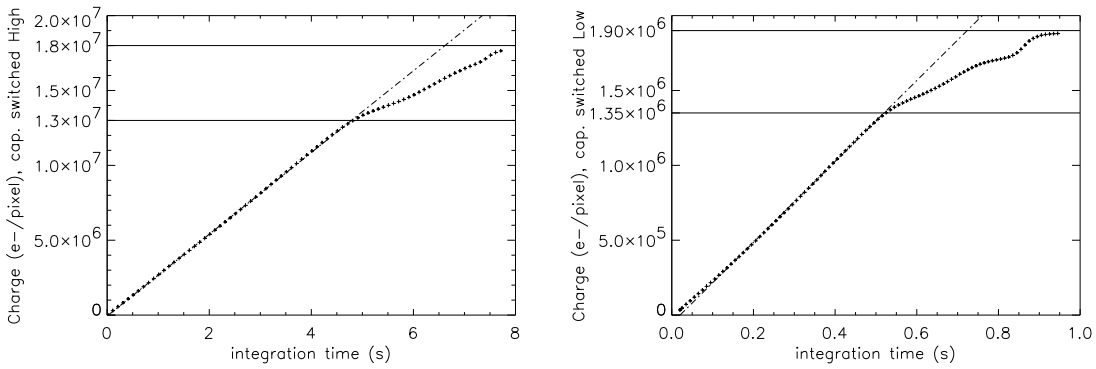

Figure 11: Linearity curve of the detector in the large (left) and small (right) capacity modes. The break in the response at $\approx 2/3$ at $1.8 \cdot 10^7$ e^- of the large and at $1.9 \cdot 10^6$ e^- of the small capacity are indicated by full lines. The top lines indicate the well capacities.

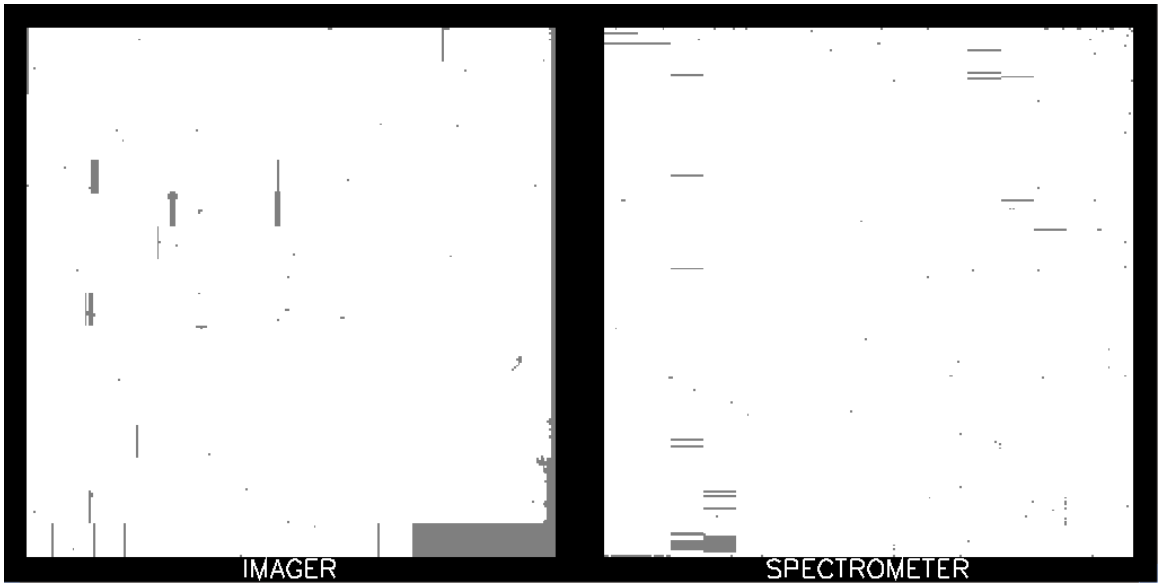

Figure 12: Bad pixel maps of the imager (left) and spectrometer (right) detectors. The large grey rectangular areas correspond to pixels masked electronically in order to decrease detector striping.

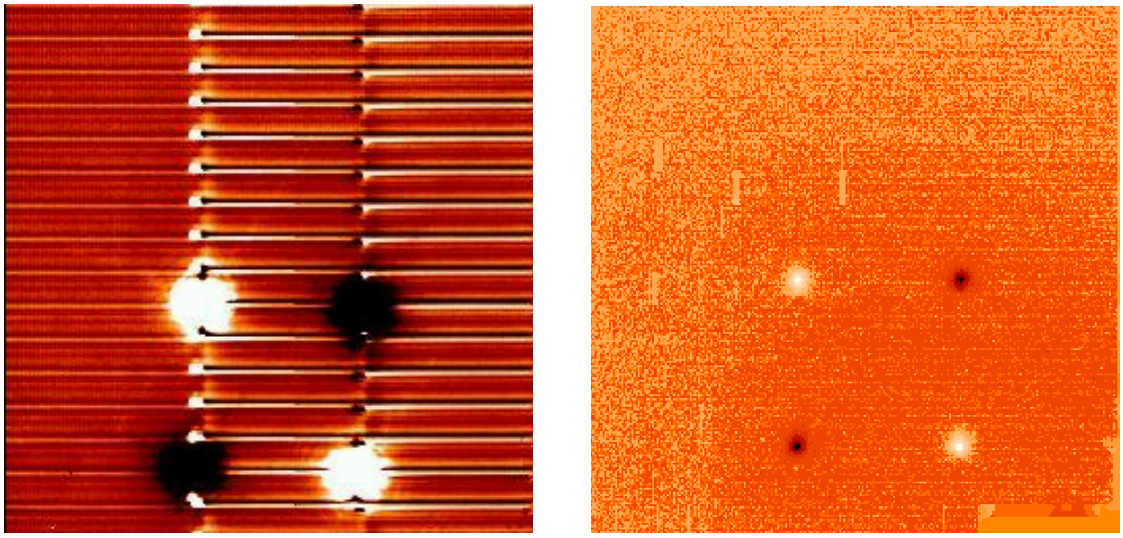

Figure 13: The DRS detector shows stripes and repeating ghosts for very bright sources (left). The ghosts are distributed every 16 columns. For other sources striping is not apparent (right).

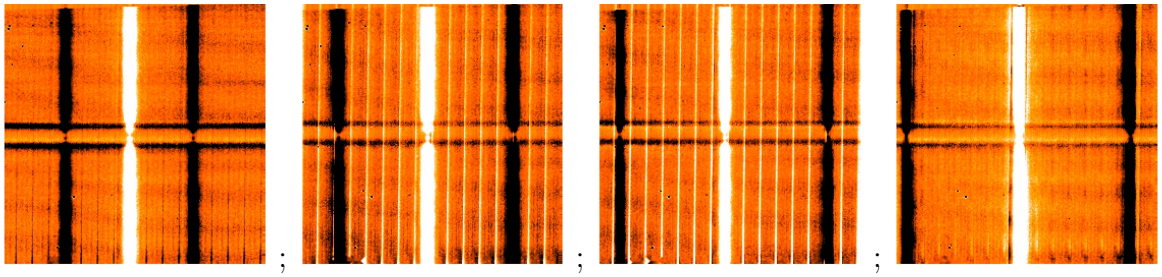

Figure 14: Sequence of chop/nod, reduced spectra obtained in the Medium Resolution mode with a central wavelength = 8.8μm . The `TEL.CHOP.THROW` = 8, 11, 13 and 14″ from left to right. Note the presence of significant striping when the 'left' beam hits some hot pixels at the lower left of the detector. For the location of the object along the slit (pixel X=123 at row Y = 128), this occured for `TEL.CHOP.THROW` between 10 and 13″, approximatively. The horizontal lines at the middle of the images are caused by the lack of detector response at 8.8μm .

of $f_{\rm chop} = 0.25\,$Hz every $T_{\rm chop} = 4\,$s one VISIR image is stored as a plane in a data cube of a FITS file. The number of chopping cycles, within one nodding position, is defined by the time spent integrating in that nodding position, $T_{\rm nod}$. This nodding period is typically $T_{\rm nod} = 90\,$s for science observations. The chopper frequency, DIT and also $T_{\rm nod}$ are predefined by the system. The number of saved A–B frames in one FITS file is:

$$\mathrm{N_{cycl_chop}} = \mathrm{T_{nod}}/\mathrm{T_{chop}} \tag{1}$$

The number of nodding cycles is computed from the total integration time as given by the observer. The total number of stacked images for each secondary position, respectively chopper half cycle, is `NDIT`. This parameter is computed according to:

$$\mathrm{NDIT} = (2 \cdot \mathrm{DIT} \cdot \mathrm{f_{chop}})^{-1} - \mathrm{NDITSKIP} \tag{2}$$

and is given by the system. It depends on `DIT`, chopping frequency and `NDITSKIP`: some read–outs at the beginning of each chopper half cycle are rejected during stabilization of the secondary. Typical stabilization times of the secondary are 25 ms. The number of rejected exposures is given by `NDITSKIP`. Similar, during stabilization after each telescope movement, respectively nodding position, a number `NCYSKIP` of chopping cycles is ignored. The timing organization of data is shown in Fig. 15.

The total on source integration time is:

$$t_{\rm source} = 4 \cdot \mathrm{N_{cycl_nod}} \cdot \mathrm{N_{cycl_chop}} \cdot \mathrm{NDIT} \cdot \mathrm{DIT} \tag{3}$$

The total rejected time is:

$$t_{\rm skip} = 4 \cdot \mathrm{N_{cycl_chop}} \cdot \mathrm{DIT} \cdot (\mathrm{NDITSKIP} \cdot \mathrm{N_{cycl_nod}} + \mathrm{NDIT} \cdot \mathrm{NCYSKIP}) \tag{4}$$

and the total observing time is:

$$t_{\rm tot} = t_{\rm source} + t_{\rm skip} \tag{5}$$

Typical duty cycles ($t_{\rm source}/t_{\rm tot}$) are about 70%.

4 Observing with VISIR at the VLT

4.1 Proposal preparation

Tools are available to prepare the observations, either during phase 1 (call for proposals), or during phase 2 (creation of observing blocks by the observer):

- The *exposure time calculator* (ETC available at http://www.eso.org/observing/etc/) may be used to estimate the integration time needed to obtain the required S/N for a given instrument setting; because of the numerous sky absorption lines, (see Fig. 20 and following), it is recommended to display the S/N as a function of wavelength when using the spectrograph ETC. This advice is particularly relevant for spectroscopic settings with wavelengths centered at 8.8μm as they will be strongly affected by the detector feature at this wavelength.

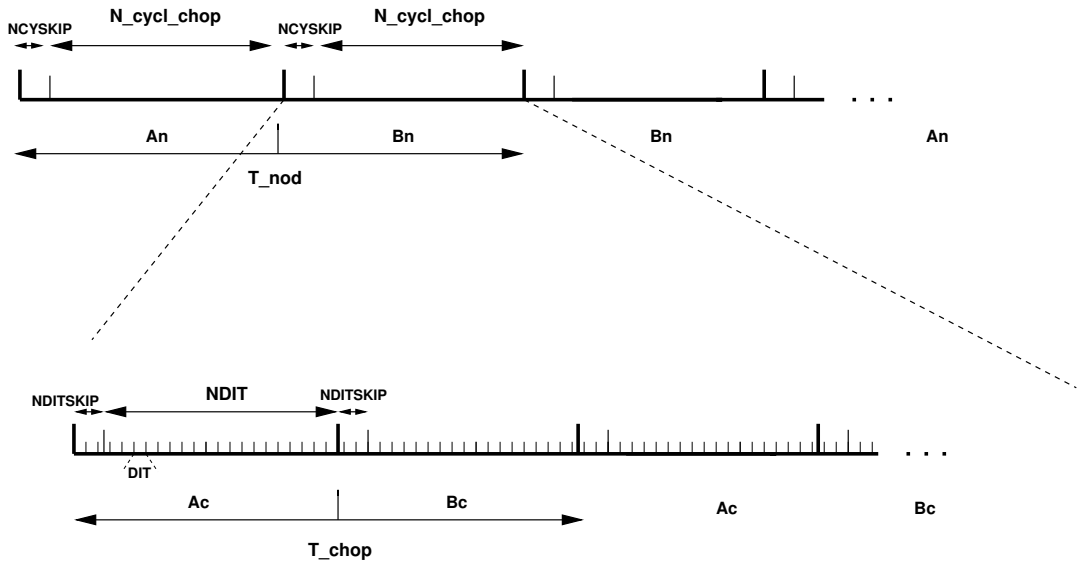

Figure 15: Data timing in VISIR. Ac and Bc refer to the two chopper positions, An and Bn refer to the two nodding (telescope) positions. Note the AnBnBnAn cycle sequence for the nodding to save observing time.

- As for all VLT instruments, astronomers with granted VISIR telescope time prepare their observations using *the phase 2 proposal preparation tool* (P2PP), described at http://www.eso.org/observing/p2pp/P2PP-tool.html. Acquisitions, observations and calibrations are coded via observing templates. One or more templates build up an observing block (OB). They contain all the information necessary for the execution of a complete observing sequence. An overview of the available VISIR templates and their parameters is given in §6 of this manual.
- For each science template, the user has to provide a finding chart so that the target can be acquired. In addition to the general instruction on how to create these finding charts, see http://www.eso.org/observing/p2pp/ServiceMode.html, the following VISIR requirements apply:
  - All finding charts have to be made using existing infrared (K-band or longer wavelength) images. Typically, 2MASS or DENIS K-band images are acceptable, although higher spatial resolution may be preferable.
  - If the wavelength at which the finding chart has been taken is different from that of the science observation, e.g. a K–band finding chart for a 10μm spectroscopic template, the user has to describe clearly how to identify the target at the observing wavelength in the README section of the programme description. Adequate examples of such comments are:
    - The target will be the brightest source in the field of view at 10μm .
    - At 10μm , there will be two bright sources in our field of view. The science target is the southernmost of these two.
- It is mandatory to check that a guide star brighter than V=13 within a field of 7.5 arcmin radius around the science target is available. This can be done using the guidecam tool (see http://www.eso.org/instruments/visir/doc). See § 4.4

Note that observations close to zenith during meridian crossing should be avoided, because of fast tracking speeds that do not allow proper background cancelation after nodding.

Questions related to the VISIR Phase1 and Phase 2 observing preparation should be directed to the User Support Department (usd-help@eso.org).

4.2 Telescope observing parameters

4.2.1 Instrument orientation on the sky

By default, the imager orientation is such that North is at the top and East is to the left. For the spectrometer, the default orientation is rotated by 90° respective to the imager, so that the North is to the left and the East to the bottom, with the slit orientation along the North-South direction.

Since VISIR is mounted on a rotator at the Cassegrain focus of Melipal, it is possible to change the default orientation of VISIR on the sky, for example, to obtain the spectra of two objects, A and B, at once. The parameter `TEL.ROT.OFFANGLE`, defaulted to 0°, is used for this purpose. If PA represents the required position angle of object B relative to A, measured on the sky east of north (i.e., counted positively from north to east) within the range 0 to 360°, then setting

$$\texttt{TEL.ROT.OFFANGLE} = 360 - \mathrm{PA}$$

allows one to have both A and B objects on the slit.

A more general case is illustrated in Figure 16. The object B is located at a Position Angle on the sky of $PA = 162°$ relative to A (see left side graph on the figure). One wishes to bring it at an apparent location on the detector indicated by the square F. The angle F–A–B, counted east of north, is $\Theta = PA + 90° = 252°$. Therefore, one needs to set

$$\texttt{TEL.ROT.OFFANGLE} = 360° - \Theta = 108°,$$

in order to obtain the requested final orientation as shown on the right side graph of Fig. 16

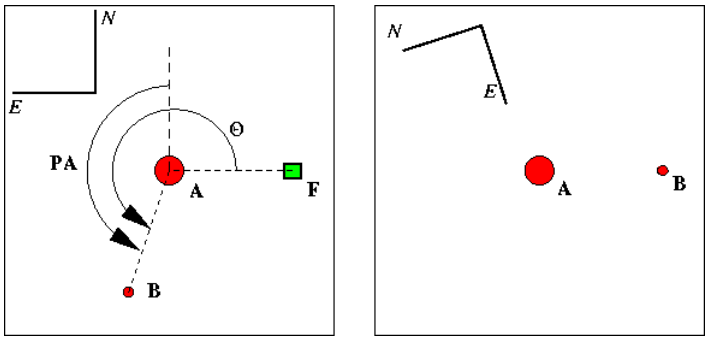

Figure 16: Setting the correct value of the `TEL.ROT.OFFANGLE` parameter. *Left side:* Object B located at a position angle $PA = 162°$ is to be brought at the apparent location F on the detector. Here, $\Theta = PA + 90$. Therefore, `TEL.ROT.OFFANGLE` $= 360° - \Theta = 108°$. *Right side:* Requested final orientation after completion of the telescope setup.

4.2.2 Chopping parameters

The chopping technique, as described in § 2, is based on beam switching using the moving secondary mirror of the telescope. It allows to alternatively observe a field, then another field

offset from the first by a chopping distance or throw, called TEL.CHOP.THROW, see Fig. 17. This parameter can be set by the user. To avoid chopping inside the object it is recommended to use a chopping and nodding throw which is $\sim$ 1.5 times larger than the estimated MIR diameter of the object. In the case of point sources, the throw is usually set around $\sim 10''$ to ensure proper separation of the different beams. The maximum chopping throw at the VLT is $30''$ and the minimum is $8''$. For good image quality, and good background cancelation, chopping and nodding throws below $15''$ are recommended (see § 4.9.1). *Note that for chopping throws larger than the field-of-view, the negative beams will not be seen on the detector, and the integration times have to be adjusted accordingly.*

The chopper position angle, PA, is the angle of chopping counted East of North (see Fig. 17). This parameter can be set by the observer. In order to keep the same distribution of beams on the detector for a different rotator angle (TEL.ROT.OFFANGLE) as in the default rotator position (see Fig. 21), then TEL.CHOP.POSANG must be equal to TEL.ROT.OFFANGLE. In particular, this is the case in spectroscopy if the observer wishes to have the 3 beams along the slit.

As stated in § 3.5, the chopping frequency is not a parameter accessible to the observer, it is fixed internally to ensure the best data quality.

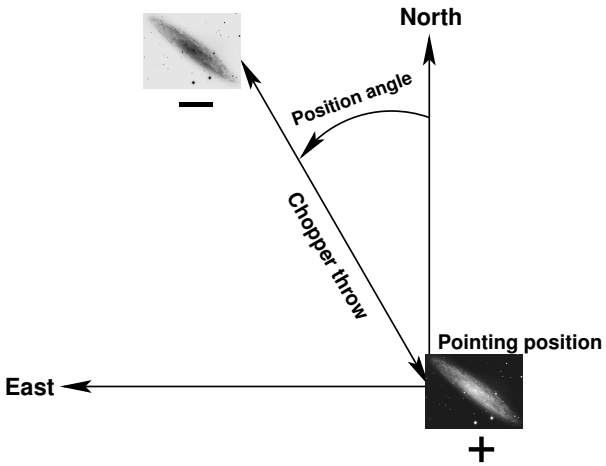

Figure 17: Definition of chopping parameters from the *telescope* point–of-view. If the position angle (PA) is measured counter–clockwise from North to East with PA between 0 and 360°, then TEL.CHOP.POSANG is $360° - PA$. The positive beam (+) is obtained when the M2 is at Chopping Position A and corresponds to the pointing position of the telescope as given in the FITS header (idle position). The negative beam (-) is obtained by moving the M2 so that it points to a position angle on the sky given by PA and a throw of TEL.CHOP.THROW from the telescope pointing position (Chopping Position B). If TEL.CHOP.POSANG = TEL.ROT.OFFANGLE $= 360° - PA$, the resulting image on the detector will appear as in one of the nodding position images illustrated in Fig. 21.

4.2.3 Nodding parameters

The nodding technique allows to switch from one field to another by offsetting the telescope by several tens of arc–seconds. It allows to correct for optical path residuals that remain after chopping (§ 2).

The nodding period is a parameter that can only be modified by the instrument operator. For exposures shorter than 180s (SEQ.TIME $< 180s$) – as possible in acquisition images–, the

nodding time is set to half the requested exposure time. For exposures longer than 180s, the nodding time is set to 90s. *In particular, exposure time given in the template will be internally changed by the software to be the closest to a multiple of 90s.*

In all the 'AutoChopNod' templates, the nodding offset is equal to `TEL.CHOP.THROW` and cannot be modified.

In order to reach Nodding Position B, the telescope executes an offset of `TEL.CHOP.THROW`, along a position angle equal to

- PA + 90° = 360° - `TEL.CHOP.POSANG` + 90°, if `SEQ.CHOPNOD.DIR` = PERPENDICULAR,
- PA + 180° = 180° - `TEL.CHOP.POSANG`, if `SEQ.CHOPNOD.DIR` = PARALLEL.

The resulting distribution of images on a frame is illustrated in Fig.21. In imaging, more flexibility on the nodding offsets are possible with the VISIR_img_obs_GenericChopNod template.

4.3 Target acquisition

4.3.1 Introduction

Observing blocks must start with an acquisition template. Pointing to a target can only be performed through an acquisition template. Target coordinate, name and proper motion are all set in the acquisition templates.

The execution of the acquisition templates presets the telescope to the target coordinates given by `TEL.TARG.ALPHA` and `TEL.TARG.DELTA`. Offsets with respect to the target coordinates can be specified by `TEL.TARG.OFFSETALPHA` and `TEL.TARG.OFFSETDELTA` and allow, for example, to use a bright offset star for precise acquisition (see Fig. 18). To guarantee proper centering within the slit when using an offset star, the angular separation between the offset star and the target should not be larger than 60″. Acquisition with an offset star has not been tested with the narrow, 0.4″ slit and should be avoided. Note that the coordinates of the target (TEL.TARG.ALPHA, TEL.TARG.DELTA) and the offsets to the reference star (TEL.TARG.OFFSETALPHA,TEL.TARG.OFFSETADELTA) must be indicated with the following convention[1] :

$$\texttt{TEL.TARG.ALPHA} + \texttt{TEL.TARG.OFFSETALPHA} = \mathrm{RA(offsetstar)},$$

$$\texttt{TEL.TARG.DELTA} + \texttt{TEL.TARG.OFFSETADELTA} = \mathrm{DEC(offsetstar)}.$$

4.3.2 Description

There are two acquisition templates for imaging, `VISIR_img_acq_Preset` and `VISIR_img_acq_MoveToPixel`. Two acquisition templates are also available for spectroscopy, `VISIR_spec_acq_MoveToSlit` and `VISIR_spec_acq_ImgMoveToSlit`. The latter one allows to perform spectroscopic acquisition with the imager detector (in intermediate field only) and therefore offers the possibility to acquire fainter objects in a larger variety of filters. The observing parameters are described in § 8.1.

The effect of all acquisition templates is first to point the telescope so that the coordinates at the center of the detector match

[1]This convention is identical to the UVES one, but differs, from example, from the ISAAC or NACO one.

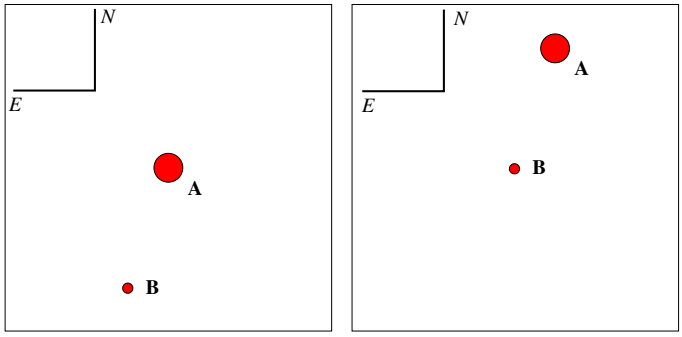

Figure 18: Setting the correct values of the TEL.TARG.OFFSETALPHA and TEL.TARG.OFFSETDELTA for a blind offset. Here the object A is a bright star used to center the target – the faint object B – at the center of the field. The telescope will first point at the object A. The instrument operator centers it properly. Once done, the telescope is offset so that object B is now properly centered and the observation templates can be executed. Following the convention described in the text, and since the target (object B) is at the east of the offset star, TEL.TARG.OFFSETALPHA is negative; on the other hand, the target is at the south of the offset star, so TEL.TARG.OFFSETDELTA is positive.

- the target coordinates, if no blind offset is used,
- the offset star coordinates, otherwise,

within the accuracy of the VLT pointing (see below). For VISIR_spec_acq_MoveToSlit, the first acquisition images are obtained with the OPEN (15.3″) slit. For VISIR_spec_acq_ImgMoveToSlit, the first acquisition images are obtained with the imager detector, Intermediate Field.
Then,

- The VISIR_img_acq_MoveToPixel, VISIR_spec_acq_MoveToSlit and VISIR_spec_acq_ImgMoveToSlit requires interaction with the instrument operator or night support astronomer in order to center the target at the appropriate location on the detector. Without further indication given by the observer, the default locations are:
  - for VISIR_img_acq_MoveToPixel and SEQ.CHOPNOD.DIR = PARALLEL: the center of the detector;
  - for VISIR_img_acq_MoveToPixel and SEQ.CHOPNOD.DIR = PERPENDICULAR: in the top left quadrant of the detector, at a distance equal to TEL.CHOP.THROW/2 from the center of the detector in both X and Y;
  - for VISIR_spec_acq_MoveToSlit: at the center of the chosen slit;
  - for VISIR_spec_acq_ImgMoveToSlit: at the center of the imager detector,

  Spectroscopic acquisition using the imager detector, with the VISIR_spec_acq_ImgMoveToSlit template, is limited to airmass smaller than 1.4 and slit witdh of 0.75 and 1.00″. In service mode, acquisition with the VISIR_spec_acq_MoveToSlit template is limited to objects brighter than 0.2 Jy.

  All acquisition images are recorded and archived. Note that, *except if specifically requested in the README file*, photometric standard stars are not necessarily observed in the same filter as the acquisition filters.

As part of the execution of the VISIR_spec_acq_MoveToSlit and VISIR_spec_acq_ImgMoveToSlit templates, an image used to measure the slit location is always taken and archived. In service mode, through slit images, obtained using the filter set by the INS.FILT2.NAME parameter, are also taken and archived so that the user can assess the correct centering of her/his object. The slit location image and the through–slit images are automatic procedures. Only the exposure time of the through–slit images can be modified by a service mode observer. Their execution time is included in the advertised execution time of the spectroscopic acquisition template.

- If the target coordinates are well known, VISIR imaging modes allow to perform blind preset observations with the VISIR_img_acq_Preset template. In this case, no acquisition images are taken.

  By default, if TEL.TARG.ALPHA and TEL.TARG.DELTA contain the (accurate) coordinates of the target, the target will be located at the center of the detector, *including if the observing templates use* SEQ.CHOPNOD.DIR = *PERPENDICULAR*. In this case, in order to avoid to lose the chopnod images, it is advisable either to

  – change the parameters TEL.TARG.ALPHA and TEL.TARG.DELTA so that they are offset by half the TEL.CHOP.THROW values, to south and west for TEL.ROT.OFFANGLE = TEL.CHOP.POSANG = 0;

  – or use the parameters TEL.TARG.OFFSETALPHA and TEL.TARG.OFFSETDELTA: as above, the convention 'final coordinates (RA, DEC) of the center of the field plus offsets equal initial coordinates' is used, which tranlates into

  $$RA + \texttt{TEL.TARG.OFFSETALPHA} = \texttt{TEL.TARG.ALPHA},$$

  $$DEC + \texttt{TEL.TARG.OFFSETDELTA} = \texttt{TEL.TARG.DELTA}.$$

  Therefore, if TEL.ROT.OFFANGLE = TEL.CHOP.POSANG = 0, TEL.TARG.OFFSETALPHA and TEL.TARG.OFFSETDELTA should be positive in order to reproduce the scheme shown in Fig. 21. A typical value for these parameters is TEL.CHOP.THROW/2, where TEL.CHOP.THROW is the chop throw used in the subsequent templates.

  If both the target and guide star coordinates are within the same astrometric systems, the pointing accuracy is limited by the relative accuracy between the coordinates of the two objects. In particular, the pointing accuracy maybe affected by significant (usually unknown) proper motion of the guide star. Note that the observatory does not guarantee the accuracy of the world coordinate systems (WCS) keywords in the FITS headers.

Acquisition with the VISIR_img_acq_MoveToPixel or VISIR_spec_acq_ImgMoveToSlit templates can make use of the K–BAND filter, for which a preliminary conservative limiting magnitude is $\sim$ 19 in 3600s on–source integration, for a S/N = 5.

For a successful completion of an OB, the observer has to ensure that correct target coordinates are provided for the equinox J2000.0 ideally at the epoch of the observations[2]. The following cases require special care:

[2]In particular, note that P2PP only accepts coordinates for J2000.0

- *imaging in the small field:* in some conditions, an error of less than $10''$ on the coordinates can bring the target outside of the field;
- *spectroscopic acquisition:* in some conditions, an error of less than $7.5''$ on the coordinates can bring the target outside of the wide slit used.

Errors of such scale are common in the following situations:

- *high proper-motion stars:* in particular, if the epoch of the VISIR observations is significantly different from the epoch for which the coordinates were determined.
- *point-like sources within extended objects:* such as an AGN: a number of catalogues do not provide accurate coordinates of the nucleus. Coordinates given by 2MASS are more reliable.
- *coordinates obtained with low spatial resolution instrument*, such as MSX, etc...

For solar system objects, the J2000.0 equinox, topocentric, ICRF or FK5 coordinates at the epoch of the observations are required, as the Telescope Control System takes into account precession, nutation, annual aberration and refraction. On the contrary, the topocentric, *apparent* coordinates at the observatory, often used in other observatories, should *not* be used. Additional velocity parameters corresponding to $\mu(\alpha)\cos\delta$ and $\mu(\delta)$ must be given in $''$/s.

4.4 Guide stars

Guide stars are mandatory for active optics and field stabilization. Any VLT programme should make sure that a guide star (USNO-A.2 or Guide Star Catalog 2) with a $V = 11-13$ mag is available within a field of 7.5' around the object.

Sensivity in the mid-IR for a ground based observatory is strongly limited by the sky brightness. In addition, the VISIR field is small compared to other VLT instruments. Therefore images of a field can often appear empty in short to medium length exposures. However, objects may become visible in longer ones. Combining different exposures taken on different nights may be tricky if a proper astrometric alignment is not carried out. Since the overall astrometric accuracy of an image is actually limited by the accuracy on the coordinates of the guide star, it is strongly recommended that all OBs of a same field use the *same* guide star, in particular for faint objects.

In addition, objects within (optically) dark molecular clouds may have few or no suitable guide stars, at least in the catalogues currently used by the Telescope Control System: the Guide Star and the USNO-A.2 catalogues. Alternatively, some bright nebulae may saturate the region of the digital sky surveys used by the telescope operator to select guide stars. Considerable amount of telescope time will be saved if such cases are identified *before* an OB is started. In these cases, examination of other catalogues, such as the USNO-B1.0, may provide suitable guide stars.

Providing the coordinates of a guide star in the acquisition template of an OB is therefore strongly recommended in a number of situations:

- observations of faint objects, hardly or not visible even after a long exposure, in particular, if this exposure has to be combined with other ones;

- observations of objects within (optically) dark molecular clouds where few suitable guide stars are expected;
- observations of objects within bright nebulae larger than the field of view accessible by the guide-probe that appeared saturated in the digital sky surveys (example: Orion);
- observations for astrometric accuracy is important.

In all these cases, the use of the guidecam tool (see http://www.eso.org/instruments/visir/doc) for VISIR is strongly recommended and the coordinates of a suitable guide star should be inserted in the acquisition templates.

If `TEL.AG.GUIDESTAR` is 'CATALOGUE', a guide star from the guide star catalog will be automatically selected by the TCS. If `TEL.AG.GUIDESTAR` is 'SETUPFILE', the observer has to provide the coordinates of the GS. The coordinates of the guide star also fix the reference point for the World Coordinate System coordinates, that appear in the FITS header of the files.

In both cases, the telescope operator acknowledges the guide star. Depending on the weather conditions or if the star appears double in the guide probe, the telescope operator may have to select another guide star. Therefore, *if the observer has selected a guide star for astrometric purposes* – for example, to insure the repeatability of the pointings between different OBs –, *a clear note should be given in the README file,* for service mode observations, *or be specifically mentioned to the night time astronomer*, in visitor mode. As stated above, the observatory does not guarantee the accuracy of the world coordinate systems (WCS) keywords in the FITS headers.

4.5 Brightness limitations

There are currently no brightness limitations with VISIR. However, it is advised to observe only sources fainter than 500 Jy in N and 2500 Jy in Q to avoid detector artifacts (§ 3.4).

4.6 Overheads

The VLT overhead for one OB which includes active optics setting, selection of guide star, field stabilization is 6 min.

VISIR instrument configurations can be changed in a short time. For example a complete change of instrument settings takes less than 2 minutes. The total time for an image acquisition of a bright sources (> 1 Jy) takes ~ 5 min. for one fine acquisition iteration, or in blind preset 2 min. Spectroscopic acquisitions take longer and are strongly dependent on the source brightness : an overhead of 15 min. is accounted for sources > 1 Jy, while 30 min. are required for sources between 0.2 and 1 Jy, respectively.

Instrument overheads due to chopping and nodding duty cycle losses have been measured to be 50% of the observing time.

The total observing time requested by the observer must include telescope and instrument overheads.

4.7 Calibration observations

MIR observations depend strongly on the ambient conditions such as humidity, temperature or airmass. In service mode science observations are interlaced by calibration observations on a timescale of 3h. Observations of photometric standards will be provided by the observatory within a time interval of three hours w.r.t. the science observations.

Calibrators, unless provided by the observer, are selected from the MIR spectro–photometric standard star catalog of the VLT (http://www.eso.org/instruments/visir). This catalog is a sub–set of the radiometric all–sky network of absolutely calibrated stellar spectra by Cohen et al.[3]. This list is supplemented by MIR standards used by TIMMI2 (see http://www.ls.eso.org/lasilla/sciops/3p6/timmi/html/stand.html).

At present the standard star catalog contains 425 sources. Zero point fluxes (Jy) have been calculated for the VISIR filter set by taking into account the measured transmission curves (Fig. 23), the detector efficiency (Fig. 9) and an atmosphere model (Fig. 1).

However, continuous observations over 3 hours of the same standar star indicates that photometric stability better than 3% can be achieved with VISIR at the VLT. In order to test if a photometric precision of the same order can be obtained, a reduced set of standard stars has been built consisting of the Cohen et al. stars which obey the following criteria:

- visibility from Paranal;
- no variability detected by Hipparcos non-variables (Var = 0 in the Hipparcos catalogue);
- absolute flux calibration errors (as reported by Cohen et al.) $< 20\%$;
- all spectral types reported in SIMBAD no more than 1 sub-class different from that used by Cohen et al.;
- not visual binaries (as reported by SIMBAD).

This catalogue of 81 stars is also made available at http://www.eso.org/instruments/visir.

From this catalogue, a further selection to provide a reduced list of 12 stars has been carried out (see also http://www.eso.org/instruments/visir). These stars are distributed as uniformly as possible in Right Ascension, with spectral types as similar as possible. In addition, their flux in the N band, of the order of 10Jy, is bright enough to be observable in the Q band without reaching non-linearity levels in the N band even in non-ideal background conditions. At least one star in this reduced catalogue will be observed every night VISIR is in use. Note that this list could be modified without previous notice.

A PSF can be derived from these photometric standard star observations. However, it is not guaranteed that its S/N is sufficient for deconvolution purposes. If the observer requires a specific PSF measurement, (s)he has to provide the corresponding PSF OB.

Observations of photometric standards provided by the observatory are taken using the `VISIR_img_cal_AutoChopNod` template (§ 6) with the following settings:

[3]Cohen et al., 1999, AJ 117, 1864

SEQ.TIME	180 sec for N and 360 sec for Q band
TEL.CHOP.POSANG	0°
TEL.CHOP.THROW	10″
SEQ.CHOPNOD.DIR	PERPENDICULAR

Filter INS.FILT1.NAME and pixel scale INS.PFOV will be set according to the science observations.

In spectroscopy, the observatory will provide spectro–photometric observations of a telluric (K or M type) standard star in the Low Resolution mode, based on the same catalog as for imaging with an airmass difference no larger than 0.2 AM respect to the science target. Such a calibration measurement will be performed at least once per night, per instrument configuration. More precisely the following settings of the VISIR_spec_cal_LRAutoChopNod template (§ 6) will be used:

SEQ.TIME	180 sec
TEL.CHOP.POSANG	0°
TEL.CHOP.THROW	8″
SEQ.CHOPNOD.DIR	PARALLEL

The wavelength setting INS.GRAT1.WLEN and INS.SLIT1.WIDTH will be adjusted to the science observation.

Important note:
The observatory does **not** provide standard calibrations for VISIR medium and high resolution spectroscopy. Thus for medium and high resolution mode the observer has to supply his own calibration by supplying a calibration OB to each science OB. The observing time needed to execute this calibration is charged to the observer. Ideally, early type stars should be chosen. In particular, for high resolution spectroscopy, asteroids provide mostly featureless spectra on the VISIR spectral range.

For both imaing and spectroscopy, day calibrations of VISIR are performed with an extended source that mimics a black–body with adjustable flux (by regulating its temperature). For most instrument modes, a corresponding flat–field is recorded, which consists of a series of images with different background levels. Exceptions are: SiC in the Intermetiate Field and all imaging obtained with the spectroscopy detector (for spectroscopy acquisition). Bad pixels, gain maps and fringing patterns can, in principle, be derived from these flat-fields. However, at the moment, the scientific value of the application of these corrections is not established. These day calibrations are supplied to the user on an experimental basis and may be discontinued with no previous notice.

4.8 OBs Classification

The sky transparency constraints used at Paranal are: photometric (PHO), clear (CLR), thin (THN), and thick (THK). They mostly refer to the optical band and their translation to the IR domain, and specially to the MIR, is not obvious. The following scheme is applied for VISIR. OBs requiring PHO conditions will be executed and classified as A if the sensitivity in the corresponding band is equal or better then the nominal median value and if the conversion

factor is constant within 10%. Refer to the web page to know the values of nominal sensitivities in each mode. OBs requiring CLR, THN and THK conditions will be executed and classified as A when the sensitivity is respectively within 20%, 30% and 50% the nominal values.

4.9 Known problems

In addition to effects caused by the cosmetic quality of the detectors mentioned above (§ 3.4), the following problems may affect the quality of the observations.

4.9.1 Decreased image quality

During the first months of VISIR operations, the image quality has been severely degraded for observations obtained with a large ($> 15''$) chopper throw. The origin of this problem has been localized and, at least for the most severe consequences, appears to be solved. However, since the solution to the problem has been applied, no tests for large chop throw ($> 25''$) in excellent optical seeing conditions have been carried out. The images shown in Fig. 19 were obtained with optical seeing at zenith of 1.2 and $1.0''$ respectively. They were obtained with `TEL.CHOP.POSANG` =270 deg and `TEL.CHOP.THROW` = 29 ″. The filter was PAH2 in the Small Field. In chop position A, the image appears symmetric, with a FWHM close to the expected limited for diffraction limited imaging. However, in chop position B, the image is affected by a coma caused by the motion of the M2, which decreases the image quality mainly in the chopping direction and adds significant structure.

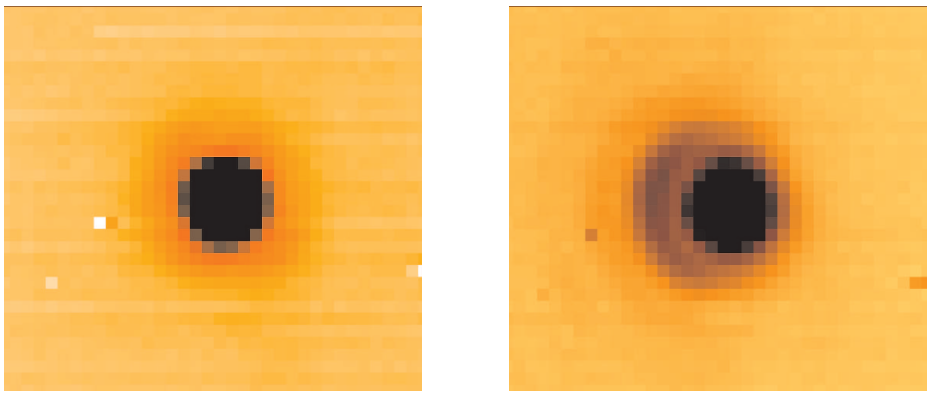

Figure 19: Image of a star obtained in the PAH2 filter in the Small Field (0.075″/pixel), and with `TEL.CHOP.THROW` = 25 ″, `SEQ.CHOPNOD.DIR` = PARALLEL and `TEL.CHOP.POSANG` = 270◦. *Left:* Chopping Position A: the image is symmetric with a FWHM close to the one expected given the optical seeing conditions. *Right:* Chopping Position B: the wings of the image shows a coma caused by the motion of M2.

4.9.2 Low–level stripes

The background level of individual DIT images fluctuates not only with the varying sky background but also with the detector temperature. The latter follows the 1Hz period of the closed–cycle cryo–coolers. The mean background level in two consecutive half–cycle frames (corresponding to the two chopper positions) may therefore not be equal. If this difference is larger than a few tens of ADUs, structures in the gain maps will appear as low–level stripes. Such stripes tend to smooth out on long integrations.

4.9.3 Bad residuals

The chopping and nodding technique does not always lead to a satisfactory removal of all the structures seen in individual images. Bad residuals have been found to occur in the following situations:

- in observations carried out close to zenith and, to a lesser extent, close to the meridian in general: the likely cause is the fast rotation of the field relative to the telescope structure;
- in variable atmospheric conditions.

In addition, it seems that imaging of extended objects are also more likely to be affected by low–level bad residuals, similar to fringes in some aspects, whose orientation on the images changes at the same angular velocity as the rotator. The origin of these structures is not understood.

4.9.4 Residuals of sky emission lines

In spectroscopy, the scanners of the grating units may still show a small residual motion at the beginning of an exposure, or, mainly for the HR or HRX modes, show some jitter after a nodding offset. The first few frames at a given wavelength setting may therefore show stronger than expected residuals at the wavelength of the sky emission lines (more exactly, of the wings of sky emission lines). For the HR and HRX modes, the residuals of the scanner jitter tend to cancel out on long integrations, and lead to a very slight decrease of the spectral resolution. An overall drift of wavelength with time has also been observed. Post-processing involving wavelength calibration of individual chopping cycles may be necessary for optimal results.

4.9.5 Fringes

The DRS detector shows fringes which are generated in the detector substrate. One example of such fringes is shown in Fig. 20 for the medium–resolution mode. The fringes are stable and are not apparent in chopped images, but the spectra are modulated. Division of the extracted spectra by standard star spectra simultaneously removes most of the fringes and corrects for telluric features.

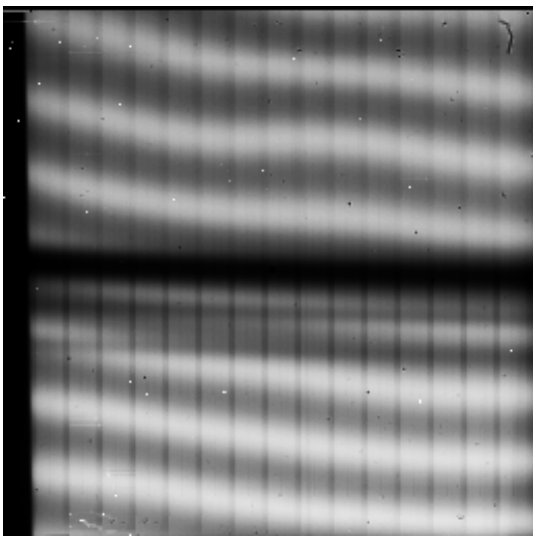

Figure 20: VISIR spectrum in staring, medium–resolution mode showing the detector fringing (white). The detector absorption feature at 8.8 μm is visible as black horizontal bar (cf. Fig. 9). Dark vertical stripes are caused by the non–uniform gain of the different electronic amplifiers. These features are largely removed by chopping.

5 VISIR data

5.1 Data format

One FITS file is saved for each telescope nodding position. This file is a data cube and contains for each chopping cycle:

1. each half cycle frame of the on–source position (A) of the chopper,
2. the average of the current and all previous(A–B) chopped frames,

In addition, the last plane of the cube contains the average of all chopped frames.

For the default value of the rotator angle (0°), images are oriented North up and East left. Spectroscopic data are aligned horizontally in the spatial and vertically in the dispersion direction (cf. Fig.20). For the LR and MR modes, the short wavelength appear at the top of the frames. For the HR and HRX modes, the short wavelength is at the top of the frame if the side *B* of the dual–grating is used, and at the bottom of the frame of the side *A* is used.

5.2 Pipeline

The VISIR pipeline has been developed by ESO/DMD and uses the ESO/CPL library. The main observation templates are supported by the pipeline reductions. Raw images of imaging and spectroscopic observations are recombined. Spectra are extracted and calibrated in wavelength (§ 5.3) for all spectroscopic modes in low–, medium–, and high–resolution. Sensitivity estimates based on standard star observations are provided both in imaging and spectroscopy (§ 4.7). Public release of the VISIR pipeline is accessible at: http://www.eso.org/instruments/visir/.

The pipeline currently supports the following templates :

- VISIR_img_obs_AutoChopNod
- VISIR_spec_obs_LRAutoChopNod
- VISIR_spec_obs_MRAutoChopNod
- VISIR_spec_obs_HRAutoChopNod
- VISIR_spec_obs_HRXAutoChopNod

In mosaic (or raster) mode (`VISIR_img_obs_GenericChopNod`) only raw frames are delivered, e.g. mapping reconstruction algorithms are not supported.

5.3 VISIR spectrometer data

Optical distortion correction

Spectra are deformed by optical distortion and slit curvatures. The VISIR spectrograph uses curved slits to cancel the distortion of the pre–slit optics. Thus the slit projected on the sky is straight. There is an additional linear distortion in both dispersion and cross–dispersion direction of the detector. The following algorithm is supported by the pipeline for low and medium resolution mode. Let us define the detector pixels in dispersion direction by x and in cross-dispersion direction by y, respectively :
a) The skew angle along x with Φ and along y with Ψ.
b) The maximum curvature along x with Δ and along y with ϵ.
Φ is defined positive in clockwise–direction and Ψ counter–clockwise; Δ is positive by increasing x and ϵ by decreasing y, respectively. Measured values of the distortion parameters are in the low and medium resolution mode $\Phi = 1.6^o$ and $\Psi = 0.7^o$. The curvatures in the low resolution mode are $\epsilon = 1.04$ pixel, $\Delta = 0.08$ pixel and for the medium resolution mode are $\epsilon = 0.26$ pixel, $\Delta = 0.08$ pixel. The center of the lower left of the detector is at (1,1). Therefore, the fix point, which is the detector center, is at (128.5, 128.5) for the n = 256 pixel array of the DRS.
The fix point is moved to (1,1) by:

$$f_1(x, y) = (x - \frac{n+1}{2}, y - \frac{n+1}{2}) \tag{6}$$

and the skew is corrected along the cross-dispersion:

$$f_2(x, y) = (x + y \cdot \tan(\Psi), y) \tag{7}$$

and along the dispersion direction:

$$f_3(x, y) = (x, y + x \cdot \tan(\Phi)) \tag{8}$$

The curvature is a segment of a circle with radius, R in x–direction given by: $n = 2\sqrt{\epsilon \cdot (2R_\epsilon - \epsilon)}$ and in y–direction by: $n = 2\sqrt{\Delta \cdot (2R_\Delta - \Delta)}$. It is corrected along the cross-dispersion:

$$f_4(x, y) = (x, y - \mathrm{sign}(\epsilon) \cdot (\mathrm{R}_\epsilon - \sqrt{\mathrm{R}_\epsilon^2 - \mathrm{x}^2})) \quad ; \quad (\epsilon \neq 0) \tag{9}$$

and along the dispersion:

$$f_5(x,y) = (x + \mathrm{sign}(\Delta) \cdot (\mathrm{R}_\Delta - \sqrt{\mathrm{R}_\Delta^2 - \mathrm{y}^2}), \mathrm{y}) \quad ; \quad (\Delta \neq 0) \tag{10}$$

Finally, the origin of the coordinate system is moved back from the fix point to (1,1):

$$f_6(x,y) = (x + \frac{n+1}{2}, y + \frac{n+1}{2}) \tag{11}$$

Spectral extraction is similar to the TIMMI2 pipeline and described by Siebenmorgen et al. 2004, AA 414, 123.

Wavelength calibration

A first order wavelength calibration is given by the optical model of the instrument. Its precision is about ±10 pixels for the low and medium resolution mode and ±15 pixels for the high resolution mode. The wavelength calibration can be refined by using Fabry-Perot Etalons plates or atmospheric lines. In the VISIR FITS file, chopper half-cycle frames, which are dominated by sky emission lines, are stored (§ 5.1). They can be used to fine–tune the wavelength calibration to sub–pixel precision by comparison with a model of the atmospheric lines. This method is used by the pipeline. More specifically, the zero–point of the wavelength calibration is obtained by cross–correlating the observed sky spectrum with a HITRAN model of the sky emission lines.

The chopped frames cannot be used for calibration with atmospheric lines because the chopping process results in a near perfect cancelation of sky lines.

Atmosphere absorption correction

The atmosphere does not uniformly absorb the MIR radiation (§ 2.1). At some wavelengths it is completely transparent, at others partly or completely opaque. Differential absorption is often corrected by dividing the extracted spectrum by a reference spectrum. This procedure may cause numerical instabilities at wavelengths close to strong sky lines that might amplify the noise.

Photometry

Spectro-photometric calibration of low and medium resolution spectra can be achieved with the MIR standard star list provided by the Observatory (see § 4.7). For high-resolution spectroscopy only calibrators known with high precision, such as, A stars or asteroids, should be considered. However, even early A stars are known to have some hydrogen absorption lines in the N and Q band.

6 VISIR templates description

6.1 Acquisition

Each OB needs to start with an acquisition template, they are described in § 4.3.

6.2 Observing with the imager

`VISIR_img_obs_AutoChopNod`

This template permits observing a source in imaging configuration with various sub-settings. The observer must specify filter, pixel scale, chopper throw, which is in the range of 8″ to 30″. The keyword `SEQ.CHOPNOD.DIR` is set to `PARALLEL` or `PERPENDICULAR`, which results in images as shown in Fig. 21. `PARALLEL` considers an equal nodding and chopping amplitude which are both in parallel direction. It is recommended for faint, extended sources, for which the spatial resolution is not so crucial. `PERPENDICULAR` considers an equal nodding and chopping amplitude; however in perpendicular direction. Note that while the telescope offset is in positive (East) direction, the resulting image on the detector will move to the West. This technique is recommended for point or relatively small extended (< 5″) sources (Fig. 4).

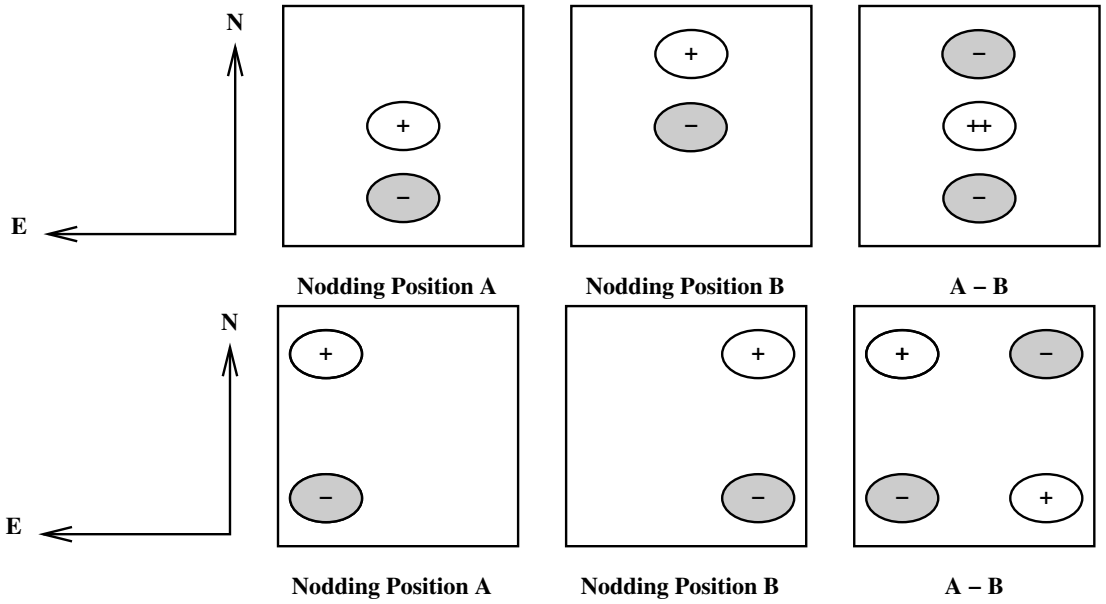

Figure 21: Schematic drawing of the content of a frame obtained with `TEL.ROT.OFFANGLE = TEL.CHOP.POSANG = 0` and `SEQ.CHOPNOD.DIR = PARALLEL` (top) and `SEQ.CHOPNOD.DIR=PERPENDICULAR` (bottom). In the individual nodding positions, the positive beams correspond to the chopper position A and the negative beams to the chopper position B. Note that the default pointing position of the telescope corresponds to the center of the detector. Within the accuracy of the telescope pointing, this location matches the nodding position A, chopper position A if `SEQ.CHOPNOD.DIR = PARALLEL`.

The keywords `SEQ.JITTER.WIDTH` allows chopping and nodding with random offsets so that a jitter pattern is performed. This technique allows to reconstruct bad pixels. For `SEQ.JITTER.WIDTH = 0` no jitter is performed and the resulting image depends on the setting of `SEQ.CHOPNOD.DIR`. The chopping period is set by the system and the nodding period is fixed to 90 s. The number

of nodding cycles N_{cycl_nod} is computed according to the total observation time (§ 3.5).

`VISIR_img_obs_GenericChopNod`
This imaging template enhances the flexibility of nodding offsets, and allows the user to specify them in a list of relative offset positions. In the most simple application, only one offset position is specified. This allows to record nodding pairs, i.e. cycle of on–off observations, using a flexible offset position. Additional jitter offsets can be specified. More than one entry in the offset list results in a freely programmable pattern of nodding pairs. Note that the integration time, `SEQ.TIME`, specified refers to only one nodding pair. The total observing time is given by the product of `SEQ.NOFF` × `SEQ.TIME`. The offset positions are calculated as the cumulative sum of offsets, i.e. are defined relative to the previous offset positions. Note that the telescope always returns to the first (reference) position, when specifying a list of offsets. This mode can be exploited to perform mosaic or raster imaging. The first reference position can then be considered as a sky observation while the offsets refer to object positions. It is recommended to offset to positions that result in observations of overlapping fields, which enhances the redundancy after image reconstruction.

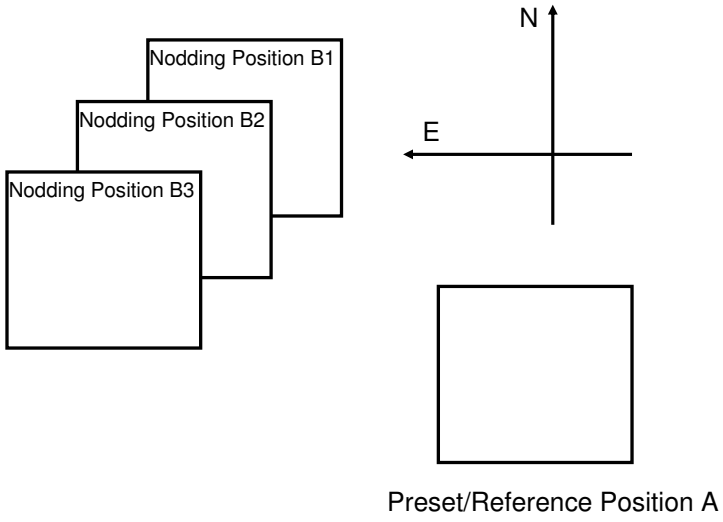

Figure 22: Illustration of generating raster maps with `VISIR_img_obs_GenericChopNod`.

An illustration of generating an raster map can be found in Fig. 22. The following parameters correspond to this setting:

```
SEQ.NOFF                    3
SEQ.OFFSET1.LIST     30 10 10
SEQ.OFFSET2.LIST    30 -10 -10
SEQ.OFFSET.COORDS         SKY
```

Note that depending on choice of the integration time `SEQ.TIME`, several nodding cycles might result, e.g. pattern like AB1B1AAB1B1A..AB2B2AAB2B2A..AB3B3AAB3B3A.

Currently, images obtained with the VISIR_img_obs_GenericChopNod are not reduced by the ESO VISIR pipeline.

Pre–imaging observations: Since Period 76, the observatory supports a fast data release for VISIR pre–imaging observations. Pre–imaging images must be obtained either with the `VISIR_img_obs_AutoChopNod` or `VISIR_img_obs_GenericChopNod` templates. The SEQ.CATG keyword must be set to PRE–IMAGE. In addition, the name of the OB must start with the prefix PRE.

6.3 Observing with the spectrometer

Conceptually the same observing techniques applies for spectroscopy as well as for imaging. The default slit orientation is in North-South direction. The length of the slit is selected by the keyword `INS.SLIT1.TYPE`: only for cross-dispersed, high-resolution, observations `SHORT` must be used, otherwise `LONG` is the default setting.

A preferred observing strategy is called "nodding on the slit", where the chopping and nodding amplitudes are small (`SEQ.CHOPNOD.DIR = PARALLEL`). Note that "nodding on the slit" requires to set the telescope rotator offset angle *and* the M2 chopping position angle to the same value (which is, in general, different from 0). This is useful to acquire two targets simultaneously in the slit.

The keyword `SEQ.JITTER.WIDTH` allows to apply random offsets *along the slit*.

More complex source geometries might require larger amplitudes, and/or `SEQ.CHOPNOD.DIR = PERPENDICULAR` in order to avoid self-cancellation.

Low and medium resolution

Templates for low and medium resolution spectroscopy are:
`VISIR_spec_obs_LRAutoChopNod` and `VISIR_spec_obs_MRAutoChopNod`, respectively. Observing parameters are: total integration time (`SEQ.TIME`), central wavelength (`INS.GRAT1.WLEN`), the slit width `INS.SLIT1.WIDTH` and `SEQ.CHOPNOD.DIR` (§ 6.2).

High resolution: long–slit mode

Template for high resolution spectroscopy is `VISIR_spc_obs_HRAutoChopNod`. Three order sorting filter at 8.02, 12.81 and 17.03μm, `INS.FILT2.NAME =` ([H2_S4],[Ne II],[H2_S1]) are available. See Table 6 for the corresponding list of offered central wavelengths. Other observing parameters are: total integration time (`SEQ.TIME`), central wavelength (`INS.GRAT1.WLEN`), the slit width (`INS.SLIT1.WIDTH`) and `SEQ.CHOPNOD.DIR` (§ 6.2).

High resolution: cross–dispersed mode

`VISIR_spc_obs_HRXAutoChopNod` is functionally similar to `VISIR_spc_obs_HRAutoChopNod`,

but uses a grism for cross-dispersion and order-separation. See Table 6 for a list of offered wavelengths. Note that the effective length of the spectrograph slit is limited to $\sim 4''$. Total integration time (`SEQ.TIME`), the slit width (`INS.SLIT1.WIDTH`) and `SEQ.CHOPNOD.DIR` are specified as usual (§ 6.2).

6.4 Calibration

Specific templates exist for the observations of photometric and spectro-photometric standard stars. They offer the same functionality as the corresponding science templates, but allow to monitor the sensitivity and image quality by observing calibration standard stars.

Their use is recommended to be properly recognized by the VISIR pipeline.

7 Checklist

This section provides a number of advice regarding the preparation of the proposal.

7.1 Phase 1

It is very important that the time justification (Box 9) of the proposal contains enough information so that its feasibility can be correctly assessed. The following points must be respected:

1. the expected S/N for each object and modes must be given;
2. in particular for extended sources: does the reported S/N refer to an area of 1 arcsec^2 (as given by the imaging ETC), to an extent of 1 arcsec in the spatial direction (as given by the spectroscopy ETC) or to the whole spatial extent of the object?
3. in spectroscopy, does the S/N refer to one pixel in the dispersion direction (as given by the ETC) or to one resolution element?
4. in case of large throw, does the S/N take into account the fact that some beams would fall outside the detector?
5. does the overhead calculation include the time required for each preset, given that OBs should in general not be longer than 1 hour?
6. is the target and mode in the GTO protected list? see: http://www.eso.org/observing/proposals/gto/
7. is there a guide star brighter than V = 13.5 mag within a radius of 7.5 arcmin around the object?

7.2 Phase 2

1. *Acquisition:* Are the coordinates accurate in the equinox J2000.0 reference frame? For high-proper motion objects, are they valid for the epoch of the observations? For solar system objects, are they in the topocentric, ICRF or FK5, J2000.0 reference frame at the epoch of the observations?
2. *Acquisition:* If the `VISIR_img_acq_Preset` is used and the following templates have `SEQ.CHOPNOD.DIR` = PERPENDICULAR, the target will appear at the center of the detector by default, with the risk of losing 3 beams that would appear outside of the field. Either slightly change the coordinates of `TEL.TARG.ALPHA` and `TEL.TARG.DELTA`, or use `TEL.TARG.OFFSETALPHA` and `TEL.TARG.OFFSETDELTA`. See § 4.3.
3. *Acquisition:* It is strongly recommended that a same guide star be selected and inserted in the acquisition template for all OBs of a same field, in particular if
   - relatively good astrometric accuracy is required;
   - the object is faint or diffuse and unlikely to be visible on short exposures;
   - the object appears in the field of a bright nebula that saturates the digitized sky survey (DSS) used by the telescope and instrument operator;

The guidecam tool (see http://www.eso.org/instruments/visir/doc) can help in selecting appropriate guide stars.

4. *Calibrations:* For calibration OBs, use the appropriate `VISIR_img_cal_AutoChopNod` or `VISIR_spc_cal_LR/MR/HR/HRXAutoChopNod` templates.

5. *Position angle:* If the observations must be carried out at a position angle different from 0, check § 4.2.1 and § 4.2.2. In particular, it is useful to clearly indicates in the README file if `TEL.CHOP.POSANG` is not equal to `TEL.ROT.OFFANGLE` to warn the instrument operator about the non-standard configuration. In particular, in spectroscopy, `TEL.CHOP.POSANG` must be equal to `TEL.ROT.OFFANGLE` in order to have the 3 beams along the slit.

8 Appendix: VISIR template parameters

8.1 Acquisition

VISIR_img_acq_MoveToPixel.tsf		
To be specified:		
Parameter	Range *(Default)*	Label
INS.FILT1.NAME	K–BAND SIC PAH1 ARIII SIV_1 SIV SIV_2 PAH2 PAH2_2 NEII_1 NEII NEII_2 Q1 Q2 Q3 *(NODEFAULT)*	Imager Filter
INS.PFOV	0.075 0.127 *(0.127)*	Imager pixel scale
SEQ.CHOPNOD.DIR	PARALLEL PERPENDICULAR *(PARALLEL)*	Relative Chop/Nod Direction
SEQ.TIME	30..3600 *(NODEFAULT)*	Total integration time (sec)
TEL.AG.GUIDESTAR	CATALOGUE SETUP-FILE NONE *(CATALOGUE)*	Get Guide Star from
TEL.CHOP.POSANG	0..359 *(0)*	Chopping Position Angle (deg)
TEL.CHOP.THROW	8..30 *(8)*	Chopping Amplitude (arcsec)
TEL.GS1.ALPHA	ra *()*	Guide star RA
TEL.GS1.DELTA	dec *()*	Guide star DEC
TEL.ROT.OFFANGLE	0..359 *(0.0)*	Rotator on Sky (=-PA on Sky)
TEL.TARG.ADDVELALPHA	*(0.0)*	RA additional tracking velocity
TEL.TARG.ADDVELDELTA	*(0.0)*	DEC additional tracking velocity
TEL.TARG.ALPHA	ra *()*	
TEL.TARG.DELTA	dec *()*	
TEL.TARG.EQUINOX	*(2000.0)*	
TEL.TARG.OFFSETALPHA	*(0.0)*	RA blind offset
TEL.TARG.OFFSETDELTA	*(0.0)*	DEC blind offset

VISIR_img_acq_Preset.tsf		
To be specified:		
Parameter	Range *(Default)*	Label
TEL.AG.GUIDESTAR	CATALOGUE SETUP-FILE NONE *(CATALOGUE)*	Get Guide Star from
TEL.GS1.ALPHA	ra *()*	Guide star RA
TEL.GS1.DELTA	dec *()*	Guide star DEC
TEL.ROT.OFFANGLE	0..359 *(0.0)*	Rotator on Sky (=-PA on Sky)
TEL.TARG.ADDVELALPHA	*(0.0)*	RA additional tracking velocity
TEL.TARG.ADDVELDELTA	*(0.0)*	DEC additional tracking velocity
TEL.TARG.ALPHA	ra *()*	
TEL.TARG.DELTA	dec *()*	
TEL.TARG.EQUINOX	*(2000.0)*	

VISIR_spec_acq_MoveToSlit.tsf		
To be specified:		
Parameter	Range *(Default)*	Label
INS.FILT2.NAME	N_SW N_LW ARIII NEII_1 NEII_2 *(NODEFAULT)*	Acquisition Filter
INS.SLIT1.TYPE	LONG SHORT *(LONG)*	Spectrometer Slit Type (long or short)
INS.SLIT1.WIDTH	0.40 0.75 1.00 *(NODEFAULT)*	Spectrometer Slit Width (arcsec)
SEQ.CHOPNOD.DIR	PARALLEL PERPENDICULAR *(PARALLEL)*	Relative Chop/Nod Direction
SEQ.TIME	30..3600 *(NODEFAULT)*	Total integration time (sec)
TEL.AG.GUIDESTAR	CATALOGUE SETUP-FILE NONE *(CATALOGUE)*	Get Guide Star from
TEL.CHOP.POSANG	0..359 *(0)*	Chopping Position Angle (deg)
TEL.CHOP.THROW	8..30 *(8)*	Chopping Amplitude (arcsec)
TEL.GS1.ALPHA	ra *()*	Guide star RA
TEL.GS1.DELTA	dec *()*	Guide star DEC
TEL.ROT.OFFANGLE	0..359 *(0.0)*	Rotator on Sky (=-PA on Sky)
TEL.TARG.ADDVELALPHA	*(0.0)*	RA additional tracking velocity
TEL.TARG.ADDVELDELTA	*(0.0)*	DEC additional tracking velocity
TEL.TARG.ALPHA	ra *()*	
TEL.TARG.DELTA	dec *()*	
TEL.TARG.EQUINOX	*(2000.0)*	
TEL.TARG.OFFSETALPHA	*(0.0)*	RA blind offset
TEL.TARG.OFFSETDELTA	*(0.0)*	DEC blind offset

VISIR_spec_acq_ImgMoveToSlit.tsf		
To be specified:		
Parameter	Range *(Default)*	Label
INS.FILT1.NAME	K–BAND SIC PAH1 ARIII SIV_1 SIV SIV_2 PAH2 PAH2_2 NEII_1 NEII NEII_2 Q1 Q2 Q3 *(NODEFAULT)*	Acquisition Filter for the imager detector
INS.FILT2.NAME	N_SW N_LW ARIII NEII_1 NEII_2 *(NODEFAULT)*	Acquisition Filter for the spectroscopy detector
INS.SLIT1.TYPE	LONG SHORT *(LONG)*	Spectrometer Slit Type (long or short)
INS.SLIT1.WIDTH	0.40 0.75 1.00 *(NODEFAULT)*	Spectrometer Slit Width (arcsec)
SEQ.CHOPNOD.DIR	PARALLEL PERPENDICULAR *(PARALLEL)*	Relative Chop/Nod Direction
SEQ.TIME	30..3600 *(NODEFAULT)*	Total integration time (sec)
TEL.AG.GUIDESTAR	CATALOGUE SETUP-FILE NONE *(CATALOGUE)*	Get Guide Star from
TEL.CHOP.POSANG	0..359 *(0)*	Chopping Position Angle (deg)
TEL.CHOP.THROW	8..30 *(8)*	Chopping Amplitude (arcsec)
TEL.GS1.ALPHA	ra *()*	Guide star RA
TEL.GS1.DELTA	dec *()*	Guide star DEC
TEL.ROT.OFFANGLE	0..359 *(0.0)*	Rotator on Sky (=-PA on Sky)
TEL.TARG.ADDVELALPHA	*(0.0)*	RA additional tracking velocity
TEL.TARG.ADDVELDELTA	*(0.0)*	DEC additional tracking velocity
TEL.TARG.ALPHA	ra *()*	
TEL.TARG.DELTA	dec *()*	
TEL.TARG.EQUINOX	*(2000.0)*	
TEL.TARG.OFFSETALPHA	*(0.0)*	RA blind offset
TEL.TARG.OFFSETDELTA	*(0.0)*	DEC blind offset

8.2 Observation

VISIR_img_obs_AutoChopNod.tsf		
To be specified:		
Parameter	Range *(Default)*	Label
INS.FILT1.NAME	K-BAND SIC PAH1 ARIII SIV_1 SIV SIV_2 PAH2 PAH2_2 NEII_1 NEII NEII_2 Q1 Q2 Q3 *(NODEFAULT)*	Imager Filter
INS.PFOV	0.075 0.127 *(0.127)*	Imager pixel scale
SEQ.CATG	PRE-IMAGE SCIENCE *(SCIENCE)*	Observation Category
SEQ.CHOPNOD.DIR	PARALLEL PERPENDICULAR *(PARALLEL)*	Relative Chop/Nod Direction
SEQ.JITTER.WIDTH	0..10 *(0)*	Random Jitter Width (arcsec)
SEQ.TIME	180..3600 *(NODEFAULT)*	Total integration time (sec)
TEL.CHOP.POSANG	0..359 *(0)*	Chopping Position Angle (deg)
TEL.CHOP.THROW	8..30 *(8)*	Chopping Amplitude (arcsec)

VISIR_img_obs_GenericChopNod.tsf		
To be specified:		
Parameter	Range *(Default)*	Label
INS.FILT1.NAME	K-BAND SIC PAH1 ARIII SIV_1 SIV SIV_2 PAH2 PAH2_2 NEII_1 NEII NEII_2 Q1 Q2 Q3 *(NODEFAULT)*	Imager Filter
INS.PFOV	0.075 0.127 *(0.127)*	Imager pixel scale
SEQ.CATG	PRE-IMAGE SCIENCE *(SCIENCE)*	Observation Category
SEQ.JITTER.WIDTH	0..10 *(0)*	Random Jitter Width (arcsec)
SEQ.NOFF	1..100 *(NODEFAULT)*	Number of offset positions
SEQ.OFFSET.COORDS	SKY DETECTOR *(NODEFAULT)*	Offset coordinates
SEQ.OFFSET1.LIST	*(NODEFAULT)*	List of offsets in RA or X
SEQ.OFFSET2.LIST	*(NODEFAULT)*	List of offsets in DEC or Y
SEQ.TIME	180..3600 *(NODEFAULT)*	Total integration time (sec)
TEL.CHOP.POSANG	0..359 *(0)*	Chopping Position Angle (deg)
TEL.CHOP.THROW	8..30 *(10)*	Chopping Amplitude (arcsec)

VISIR_spec_obs_LRAutoChopNod.tsf		
To be specified:		
Parameter	Range *(Default)*	Label
INS.GRAT1.WLEN	8.1 8.5 8.8 9.8 11.4 12.2 12.4 *(NODEFAULT)*	Spectrometer Wavelength (microns)
SEQ.CHOPNOD.DIR	PARALLEL PERPENDICULAR *(PARALLEL)*	Relative Chop/Nod Direction
SEQ.JITTER.WIDTH	0..10 *(0)*	Random Jitter Width (arcsec)
SEQ.TIME	180..3600 *(NODEFAULT)*	Total integration time (sec)
TEL.CHOP.POSANG	0..359 *(0)*	Chopping Position Angle (deg)
TEL.CHOP.THROW	8..30 *(8)*	Chopping Amplitude (arcsec)

VISIR_spec_obs_MRAutoChopNod.tsf		
To be specified:		
Parameter	Range *(Default)*	Label
INS.GRAT1.WLEN	7.5..28.08 *(NODEFAULT)*	Spectrometer Wavelength (microns)
SEQ.CHOPNOD.DIR	PARALLEL PERPENDICULAR *(PARALLEL)*	Relative Chop/Nod Direction
SEQ.JITTER.WIDTH	0..10 *(0)*	Random Jitter Width (arcsec)
SEQ.TIME	180..3600 *(NODEFAULT)*	Total integration time (sec)
TEL.CHOP.POSANG	0..359 *(0)*	Chopping Position Angle (deg)
TEL.CHOP.THROW	8..30 *(8)*	Chopping Amplitude (arcsec)

VISIR_spec_obs_HRAutoChopNod.tsf		
To be specified:		
Parameter	Range *(Default)*	Label
INS.FILT2.NAME	NEII_2 H2S_1 H2S_4 *(NEII_2)*	Spectrometer Filter
INS.GRAT1.WLEN	7.80..19.18 *(12.810)*	Spectrometer Wavelength (microns)
SEQ.CHOPNOD.DIR	PARALLEL PERPENDICULAR *(PARALLEL)*	Relative Chop/Nod Direction
SEQ.JITTER.WIDTH	0..10 *(0)*	Random Jitter Width (arcsec)
SEQ.TIME	180..3600 *(NODEFAULT)*	Total integration time (sec)
TEL.CHOP.POSANG	0..359 *(0)*	Chopping Position Angle (deg)
TEL.CHOP.THROW	8..30 *(8)*	Chopping Amplitude (arcsec)

VISIR_spec_obs_HRXAutoChopNod.tsf		
To be specified:		
Parameter	Range *(Default)*	Label
INS.GRAT1.WLEN	7.60..28.08 *(NODEFAULT)*	Spectrometer Wavelength (microns)
SEQ.CHOPNOD.DIR	PARALLEL PERPENDICULAR *(PARALLEL)*	Relative Chop/Nod Direction
SEQ.JITTER.WIDTH	0..10 *(0)*	Random Jitter Width (arcsec)
SEQ.TIME	180..3600 *(NODEFAULT)*	Total integration time (sec)
TEL.CHOP.POSANG	0..359 *(0)*	Chopping Position Angle (deg)
TEL.CHOP.THROW	8..30 *(8)*	Chopping Amplitude (arcsec)

8.3 Calibration

VISIR_img_cal_AutoChopNod.tsf		
To be specified:		
Parameter	Range *(Default)*	Label
INS.FILT1.NAME	K-BAND SIC PAH1 ARIII SIV_1 SIV SIV_2 PAH2 PAH2_2 NEII_1 NEII NEII_2 Q1 Q2 Q3 *(NODEFAULT)*	Imager Filter
INS.PFOV	0.075 0.127 *(0.127)*	Imager pixel scale
SEQ.CHOPNOD.DIR	PARALLEL PERPENDICULAR *(PERPENDICULAR)*	Relative Chop/Nod Direction
SEQ.JITTER.WIDTH	0..10 *(0)*	Random Jitter Width (arcsec)
SEQ.TIME	30..3600 *(NODEFAULT)*	Total integration time (sec)
TEL.CHOP.POSANG	0..359 *(0)*	Chopping Position Angle (deg)
TEL.CHOP.THROW	8..30 *(8)*	Chopping Amplitude (arcsec)

VISIR_spec_cal_LRAutoChopNod.tsf		
To be specified:		
Parameter	Range *(Default)*	Label
INS.GRAT1.WLEN	8.1 8.5 8.8 9.8 11.4 12.2 12.4 *(NODEFAULT)*	Spectrometer Wavelength (microns)
SEQ.CHOPNOD.DIR	PARALLEL PERPENDICULAR *(PARALLEL)*	Relative Chop/Nod Direction
SEQ.JITTER.WIDTH	0..10 *(0)*	Random Jitter Width (arcsec)
SEQ.TIME	30..3600 *(NODEFAULT)*	Total integration time (sec)
TEL.CHOP.POSANG	0..359 *(0)*	Chopping Position Angle (deg)
TEL.CHOP.THROW	8..30 *(8)*	Chopping Amplitude (arcsec)

VISIR_spec_cal_MRAutoChopNod.tsf		
To be specified:		
Parameter	Range *(Default)*	Label
INS.GRAT1.WLEN	7.5..28.08 *(NODEFAULT)*	Spectrometer Wavelength (microns)
SEQ.CHOPNOD.DIR	PARALLEL PERPENDICULAR *(PARALLEL)*	Relative Chop/Nod Direction
SEQ.JITTER.WIDTH	0..10 *(0)*	Random Jitter Width (arcsec)
SEQ.TIME	30..3600 *(NODEFAULT)*	Total integration time (sec)
TEL.CHOP.POSANG	0..359 *(0)*	Chopping Position Angle (deg)
TEL.CHOP.THROW	8..30 *(8)*	Chopping Amplitude (arcsec)

VISIR_spec_cal_HRAutoChopNod.tsf		
To be specified:		
Parameter	Range *(Default)*	Label
INS.FILT2.NAME	NEII_2 H2S_1 H2S_4 *(NEII_2)*	Spectrometer Filter
INS.GRAT1.WLEN	7.80..19.18 *(12.810)*	Spectrometer Wavelength (microns)
SEQ.CHOPNOD.DIR	PARALLEL PERPENDICULAR *(PARALLEL)*	Relative Chop/Nod Direction
SEQ.JITTER.WIDTH	0..10 *(0)*	Random Jitter Width (arcsec)
SEQ.TIME	30..3600 *(NODEFAULT)*	Total integration time (sec)
TEL.CHOP.POSANG	0..359 *(0)*	Chopping Position Angle (deg)
TEL.CHOP.THROW	8..30 *(8)*	Chopping Amplitude (arcsec)

VISIR_spec_cal_HRXAutoChopNod.tsf		
To be specified:		
Parameter	Range *(Default)*	Label
INS.GRAT1.WLEN	7.60..28.08 *(NODEFAULT)*	Spectrometer Wavelength (microns)
SEQ.CHOPNOD.DIR	PARALLEL PERPENDICULAR *(PARALLEL)*	Relative Chop/Nod Direction
SEQ.JITTER.WIDTH	0..10 *(0)*	Random Jitter Width (arcsec)
SEQ.TIME	30..3600 *(NODEFAULT)*	Total integration time (sec)
TEL.CHOP.POSANG	0..359 *(0)*	Chopping Position Angle (deg)
TEL.CHOP.THROW	8..30 *(8)*	Chopping Amplitude (arcsec)

9 Appendix: Filter transmission curves

The filter transmission has been measured using a Fourier Transform Spectrometer, at a temperature of 35 K for filters manufactured by the company READING. Their absolute transmission curves are displayed in Fig. 23. The other filters, manufactured by OCLI, have been measured using the WCU and wavelength scans with the monochromator. Note that for these filters, the transmission curves are normalized to 1, see Fig. 19.

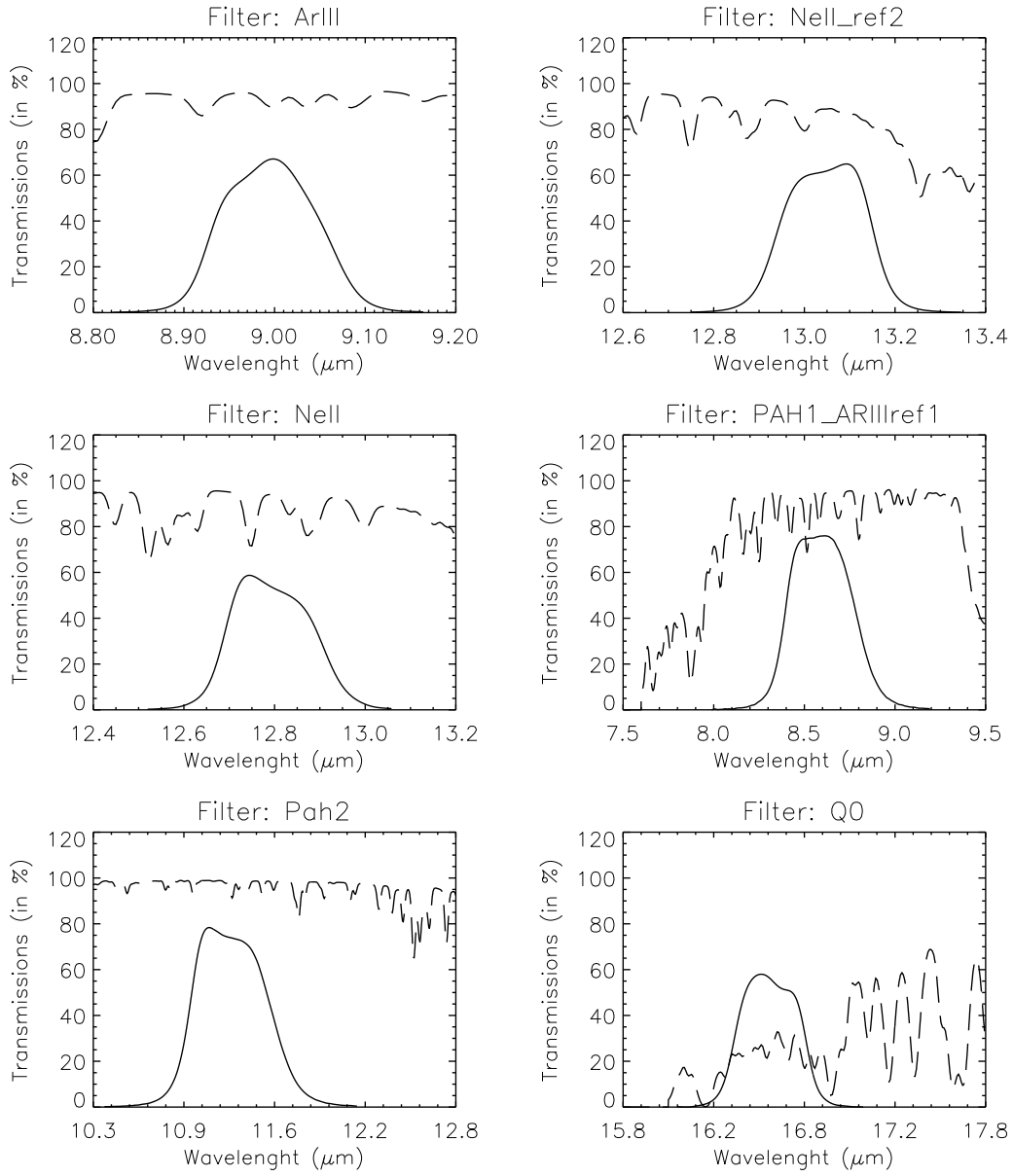

Figure 23: Transmission curves of VISIR imager filters, manufactured by READING. Overplotted (dashed) is the atmospheric transmission at low resolution. The absolute transmission values are given, expressed in percent.

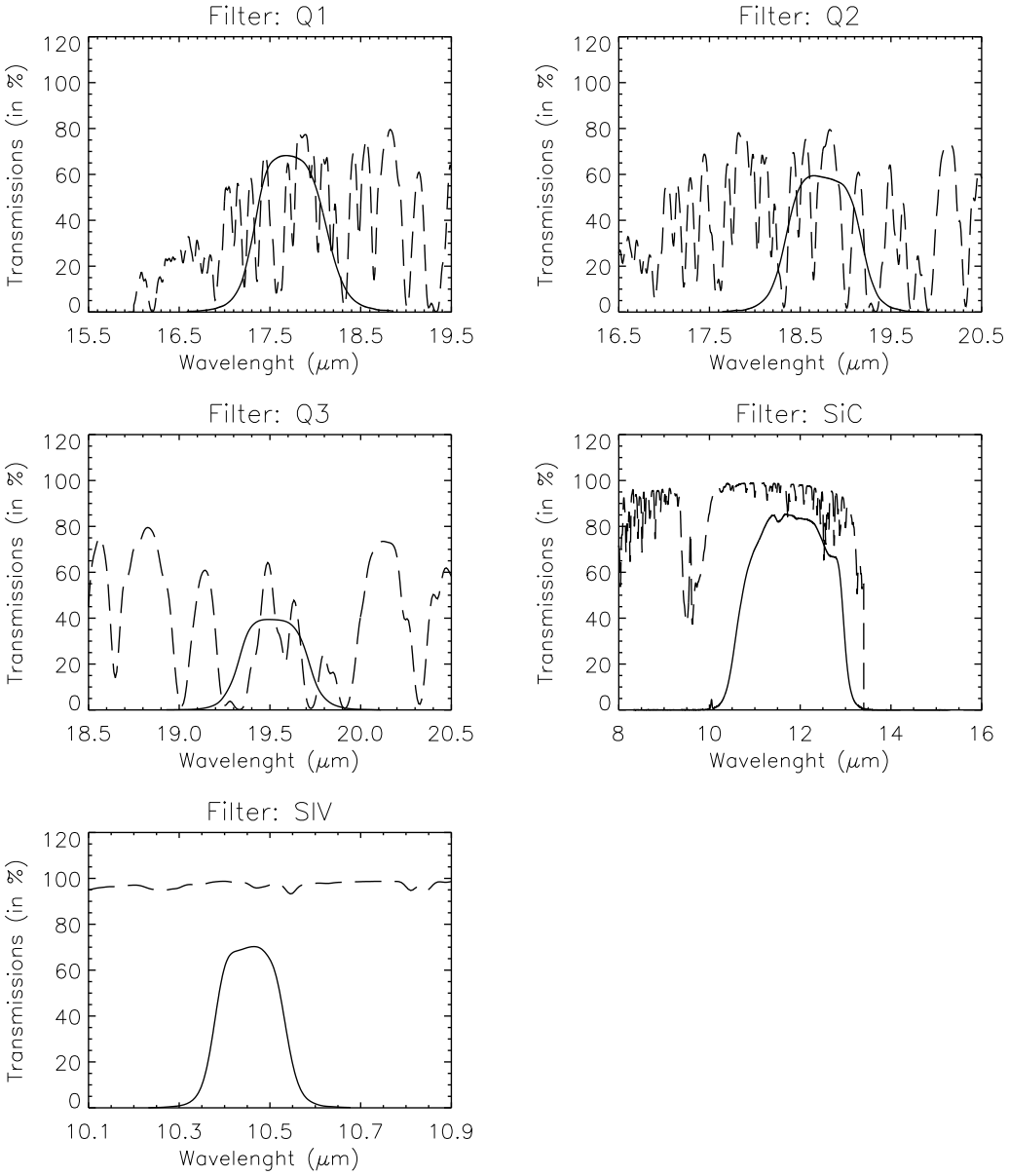

Figure 18: – continued.

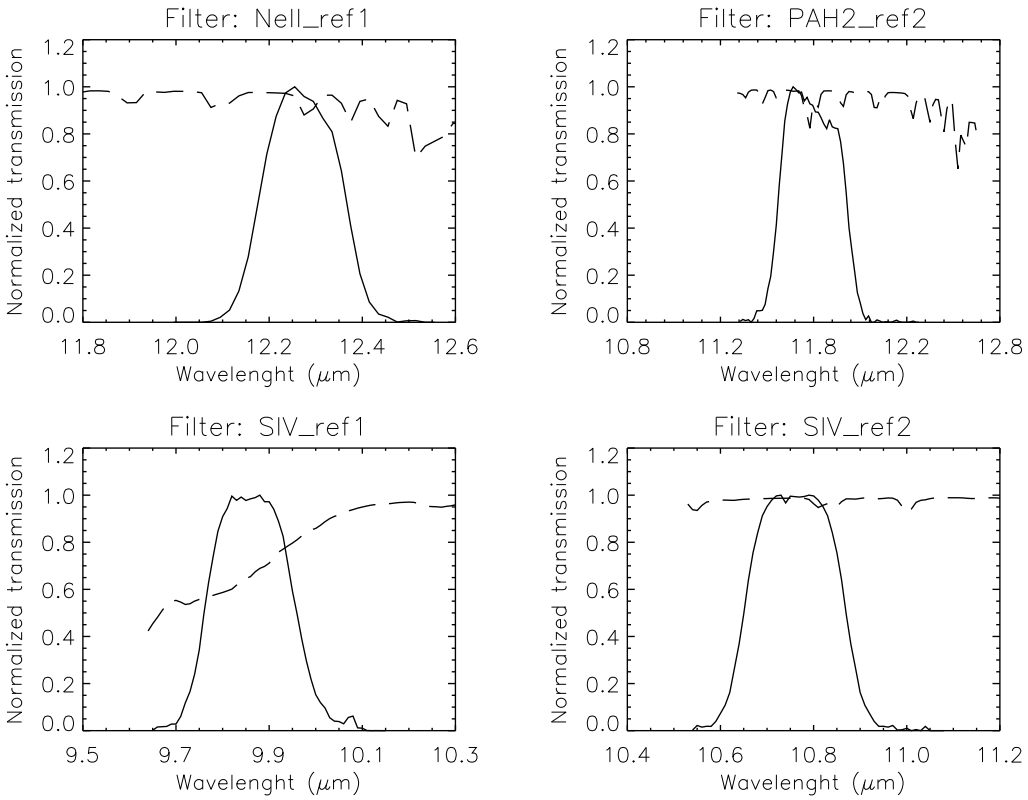

Figure 19: Transmission curves of VISIR imager filters, manufactured by OCLI. Overplotted (dashed) is the atmospheric transmission at low resolution. Only relative transmissions have been determined; their values are normalized so that their peak transmission is equal to 1.

10 Appendix: Observed sensitivities in various spectroscopic settings

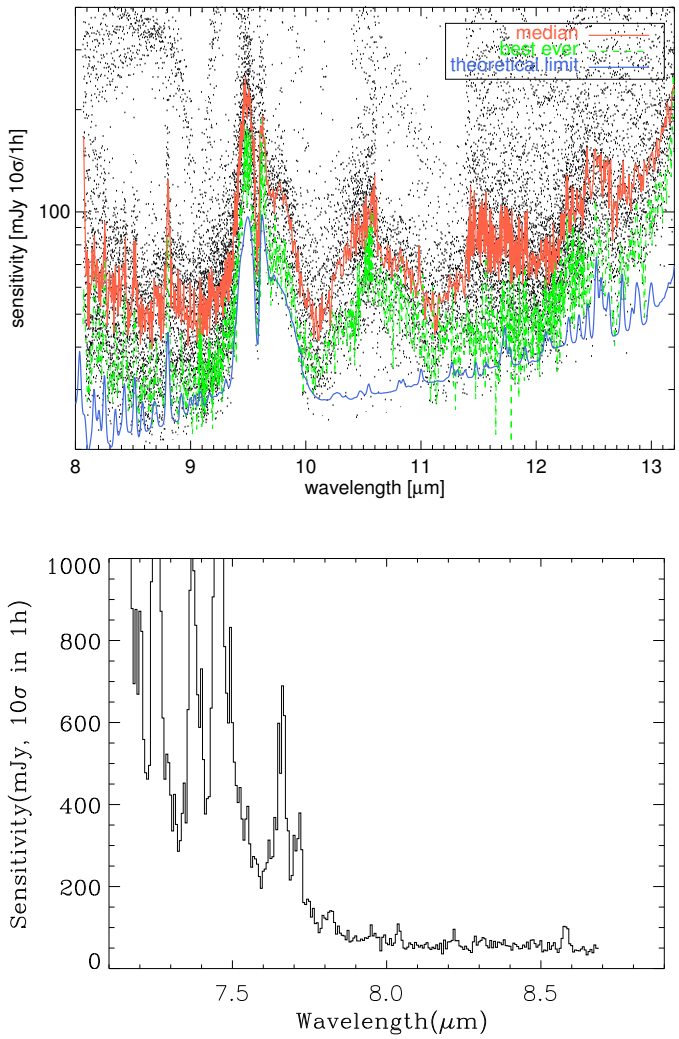

Figure 20: Sensitivity as a function of wavelength for low resolution mode. *Top:* Four offered settings of the N-band low-resolution are stitched together. Atmospheric molecular absorption, e.g. at 9.55, 11.8 and 12.5 μm, is evident. Note the detector feature at 8.8 μm. Dots indicate individual observations, full lines represent median and the dashed line the best sensitivities. Theoretical model curves correspond to BLIP. *Bottom:* Sensitivity measured in the bluer setting, centered at 8.1μm .

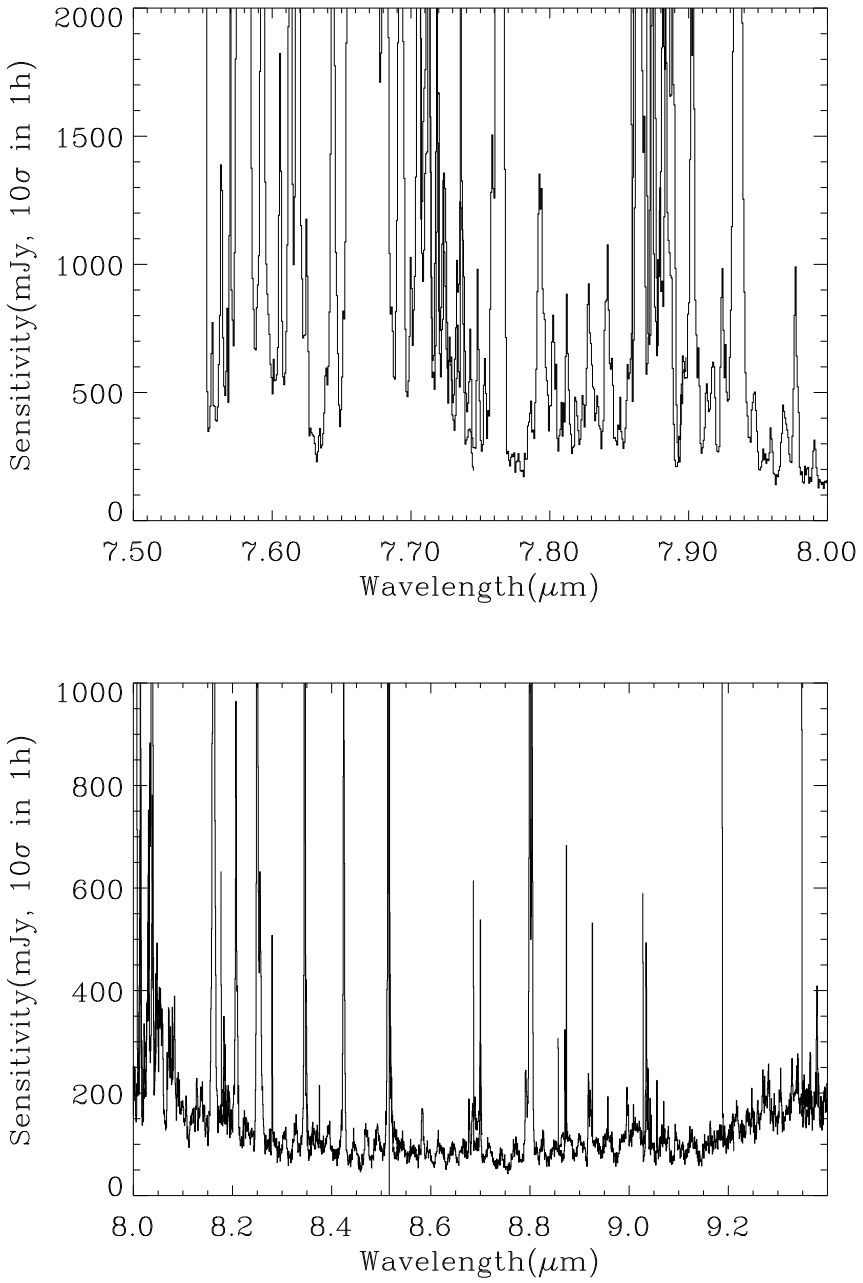

Figure 21: Observed sensitivity as a function of wavelength for different settings in the medium resolution mode obtained in very good weather conditions: (I) for $7.5\mu\text{m} < \lambda < 9.4\mu\text{m}$. Offered sensitivity is typically a factor of 2 larger.

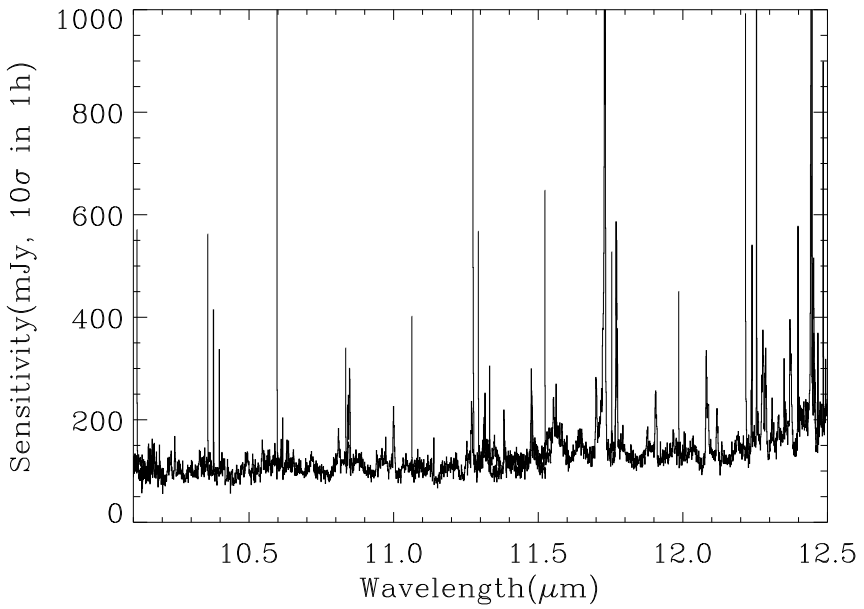

Figure 22: Observed sensitivity as a function of wavelength for different settings in the medium resolution mode obtained in very good weather conditions: (II) for $10.1\mu\text{m} < \lambda < 12.5\mu\text{m}$. Offered sensitivity is typically a factor of 2 larger.

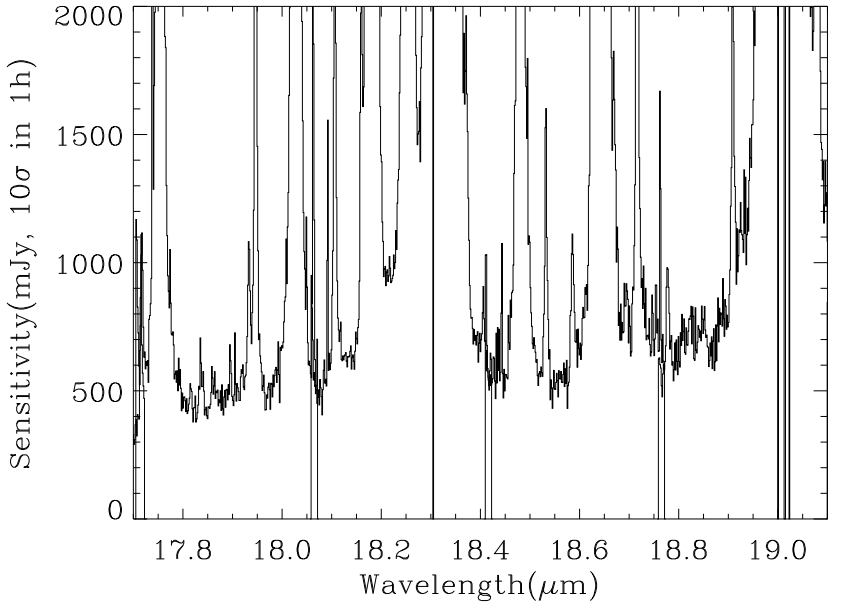

Figure 23: Observed sensitivity as a function of wavelength for different settings in the medium resolution mode obtained in very good weather conditions: (III) for $17.7\mu\text{m} < \lambda < 19.1\mu\text{m}$. Offered sensitivity is typically a factor of 2 larger.

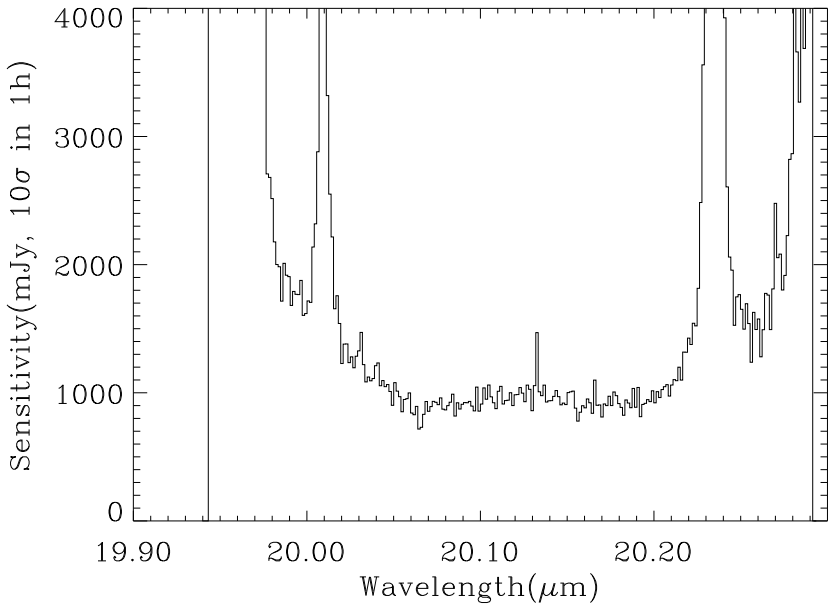

Figure 24: Observed sensitivity as a function of wavelength for different settings in the medium resolution mode obtained in very good weather conditions: (IV) for $19.9\mu\text{m} < \lambda < 20.3\mu\text{m}$. Offered sensitivity is typically a factor of 2 larger.

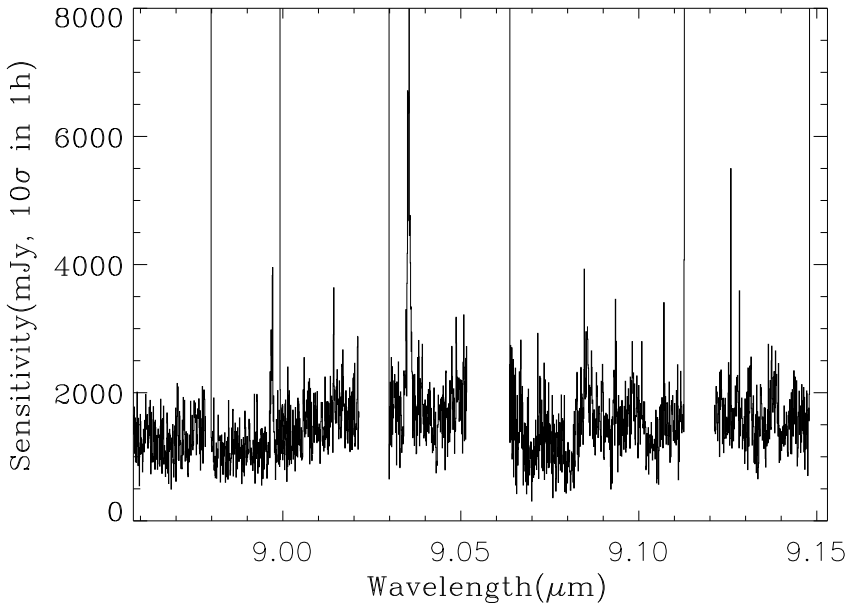

Figure 25: Observed sensitivity as a function of wavelength for high resolution mode. Offered sensitivity is typically a factor of 2 larger.

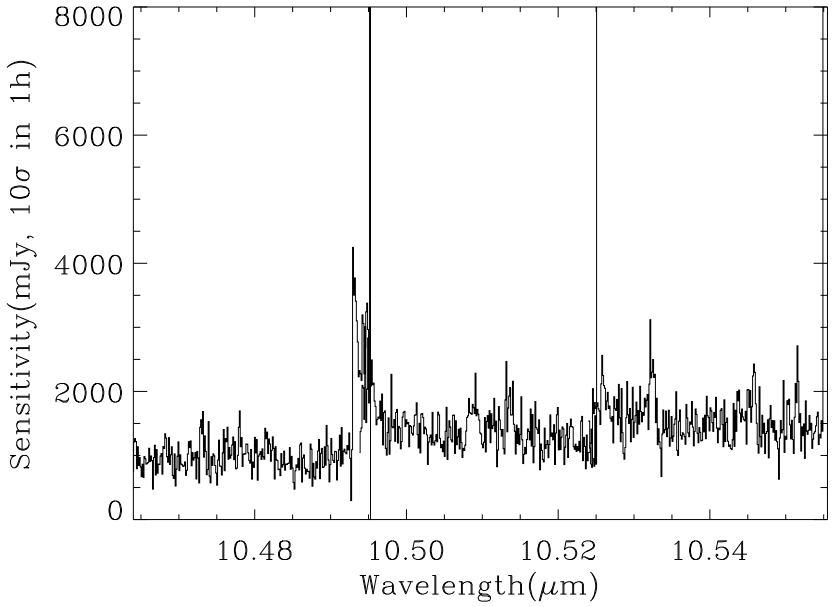

Figure 26: Observed sensitivity as a function of wavelength for high resolution mode. Offered sensitivity is typically a factor of 2 larger.

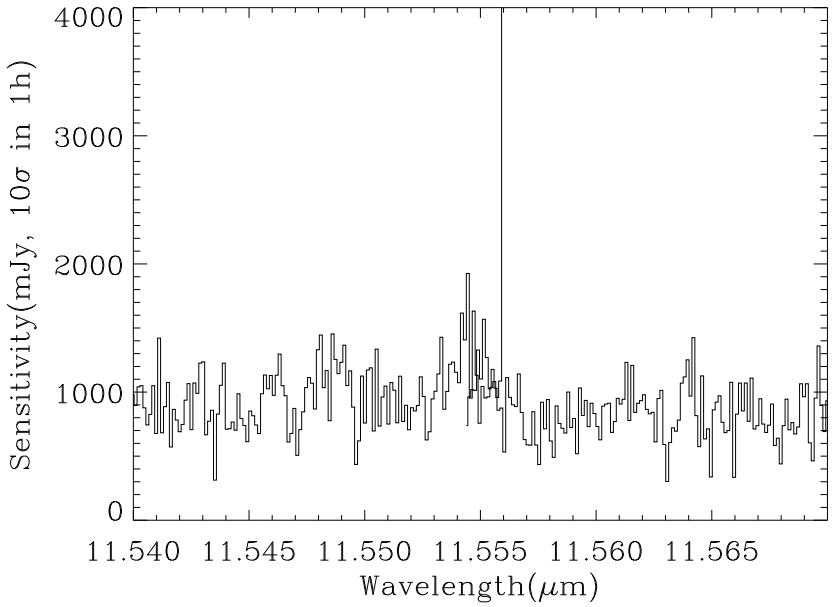

Figure 27: Observed sensitivity as a function of wavelength for high resolution mode. Offered sensitivity is typically a factor of 2 larger.

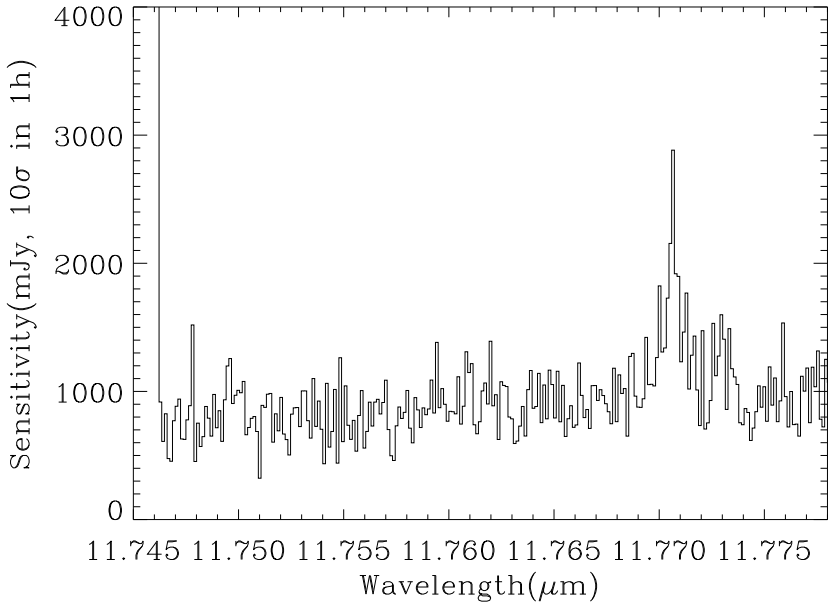

Figure 28: Observed sensitivity as a function of wavelength for high resolution mode. Offered sensitivity is typically a factor of 2 larger.

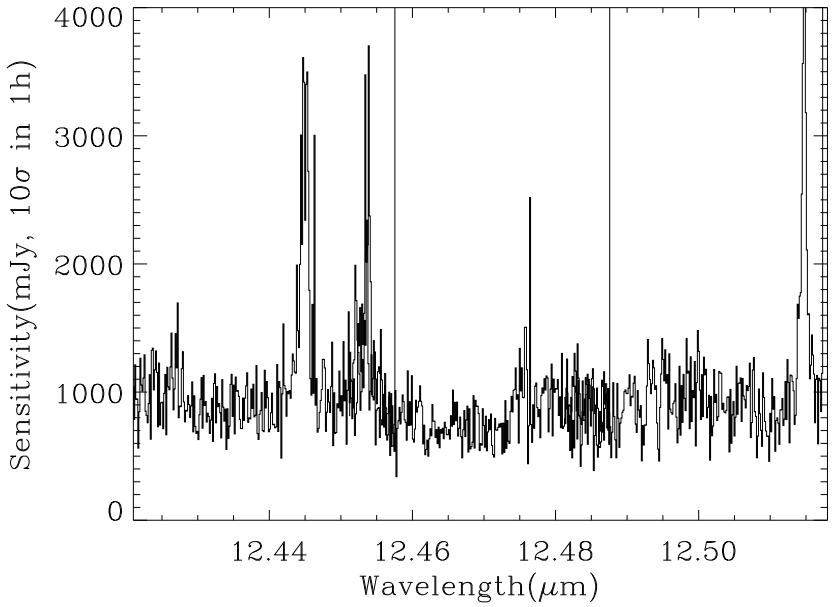

Figure 29: Observed sensitivity as a function of wavelength for high resolution mode. Offered sensitivity is typically a factor of 2 larger.

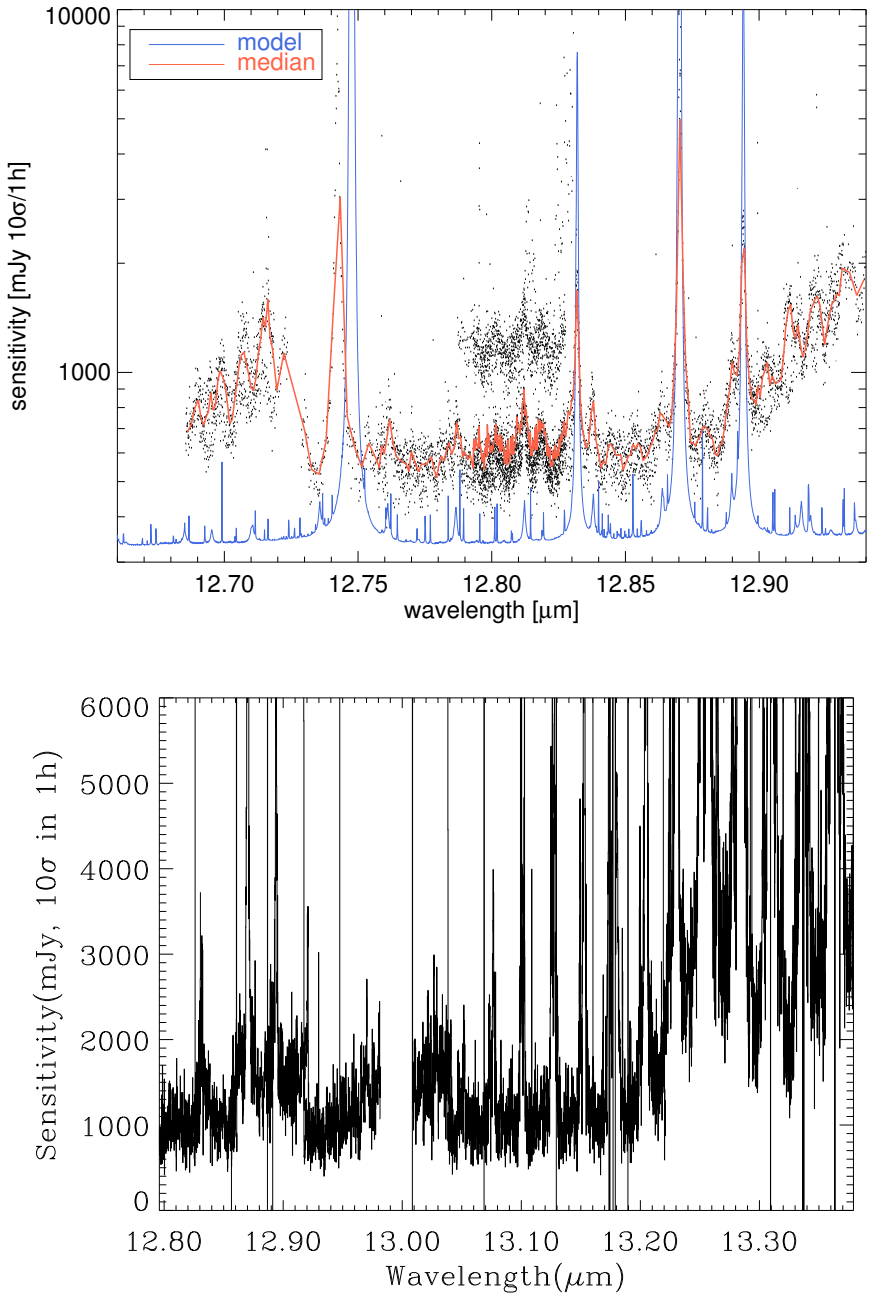

Figure 30: Observed sensitivity as a function of wavelength for high resolution mode. *Top:* Observed sensitivities obtained on various nights, compared with the theoretical model curves, corresponding to BLIP. *Bottom:* Sensitivities over an extended region encompassing the observed wavelengtgh of [NeII] up to $z \approx 0.038$.

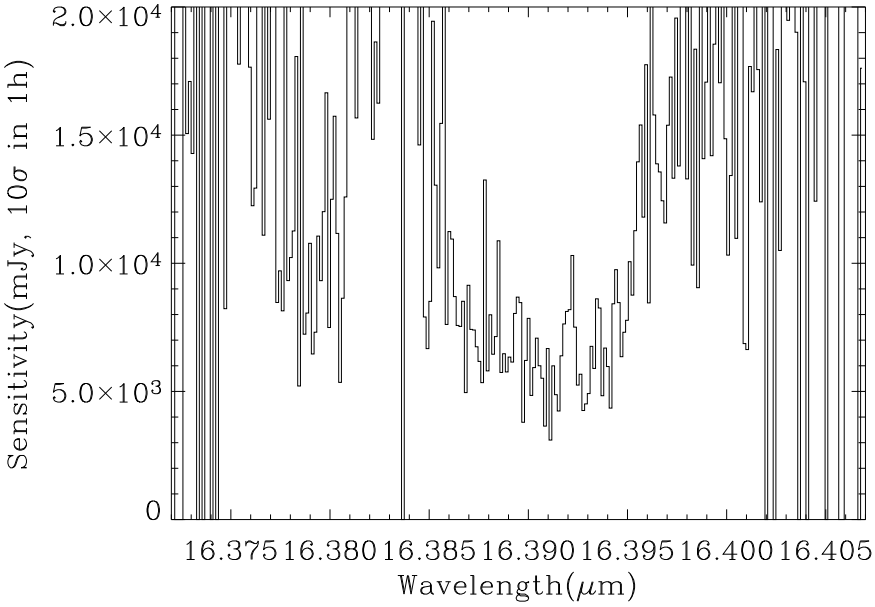

Figure 31: Observed sensitivity as a function of wavelength for high resolution mode. Offered sensitivity is typically a factor of 2 larger.

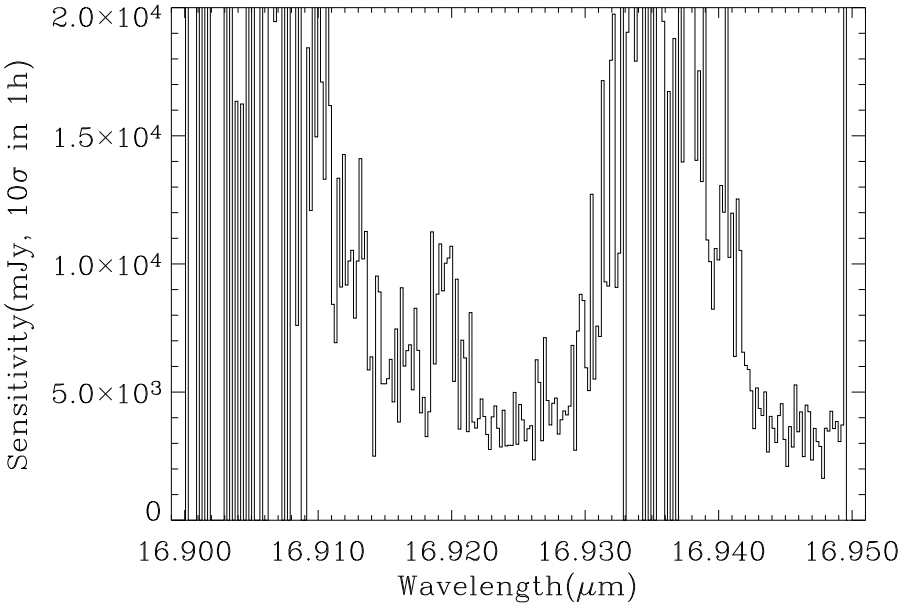

Figure 32: Observed sensitivity as a function of wavelength for high resolution mode. Offered sensitivity is typically a factor of 2 larger.

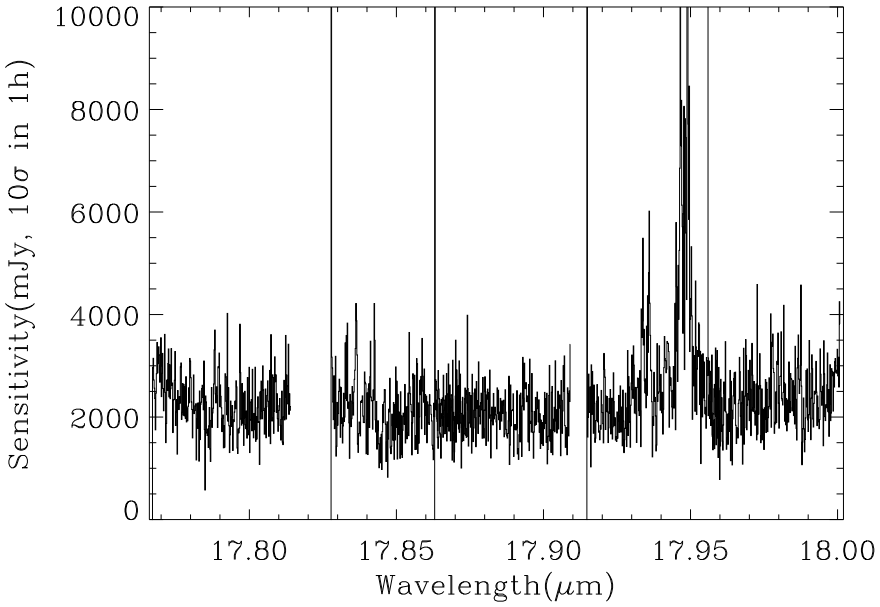

Figure 33: Observed sensitivity as a function of wavelength for high resolution mode. Offered sensitivity is typically a factor of 2 larger.

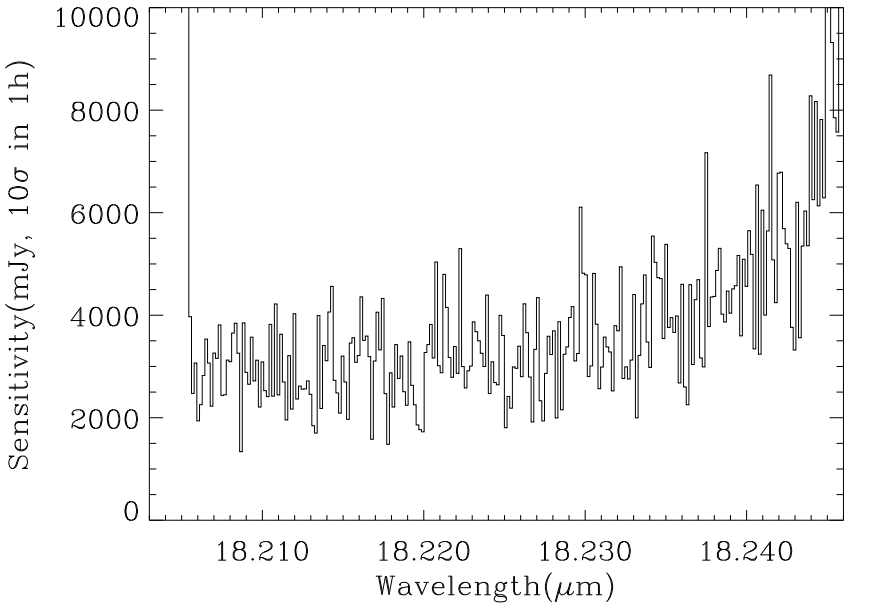

Figure 34: Observed sensitivity as a function of wavelength for high resolution mode. Offered sensitivity is typically a factor of 2 larger.

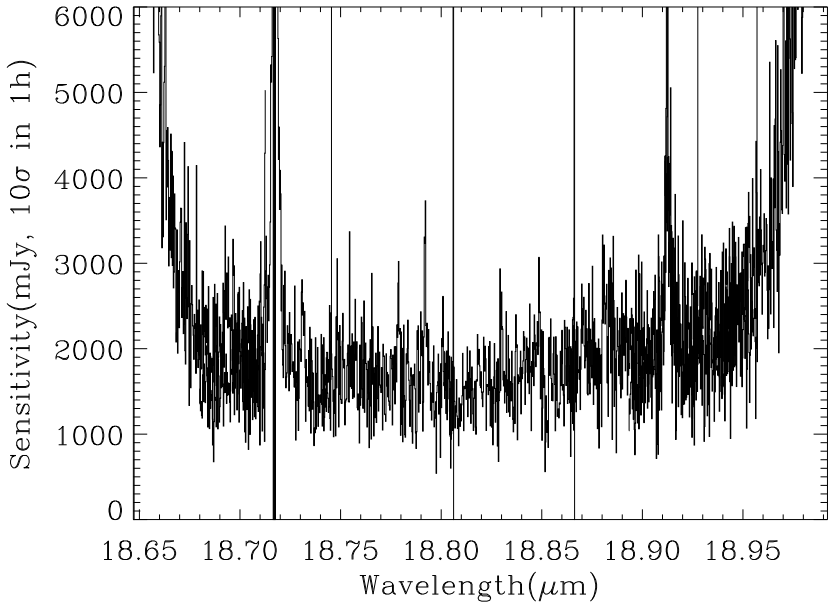

Figure 35: Observed sensitivity as a function of wavelength for high resolution mode. Offered sensitivity is typically a factor of 2 larger.

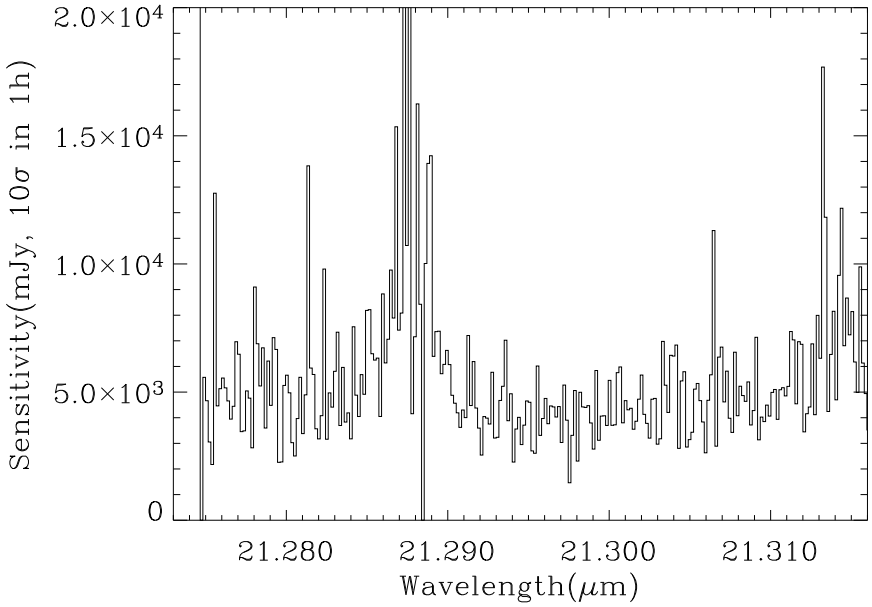

Figure 36: Observed sensitivity as a function of wavelength for high resolution mode. Offered sensitivity is typically a factor of 2 larger.